Accepted Manuscript

Structural Controls on gold mineralization on the margin of the Yilgarn craton, Albany–Fraser orogen: The Tropicana Deposit, Western Australia

T.G. Blenkinsop, M.G. Doyle

PII: S0191-8141(14)00026-1

DOI: 10.1016/j.jsg.2014.01.013

Reference: SG 3017

To appear in: *Journal of Structural Geology*

Received Date: 1 March 2013

Revised Date: 20 January 2014

Accepted Date: 26 January 2014

Please cite this article as: Blenkinsop, T.G., Doyle, M.G., Structural Controls on gold mineralization on the margin of the Yilgarn craton, Albany–Fraser orogen: The Tropicana Deposit, Western Australia, *Journal of Structural Geology* (2014), doi: 10.1016/j.jsg.2014.01.013.

- Tropicana is a world class gold deposit on the margin of the Yilgarn craton
- Gold was precipitated in the Archean at greenschist facies within granulite gneiss hosts
- Mineralization was governed by fluid flow in a network of shear zones
- The shear zones and ore bodies reflect the geometry of the host gneisses
- The entire history of five deformation events has affected gold mineralization

Gneissic banding and shear planes have similar orientations and control ore bodies

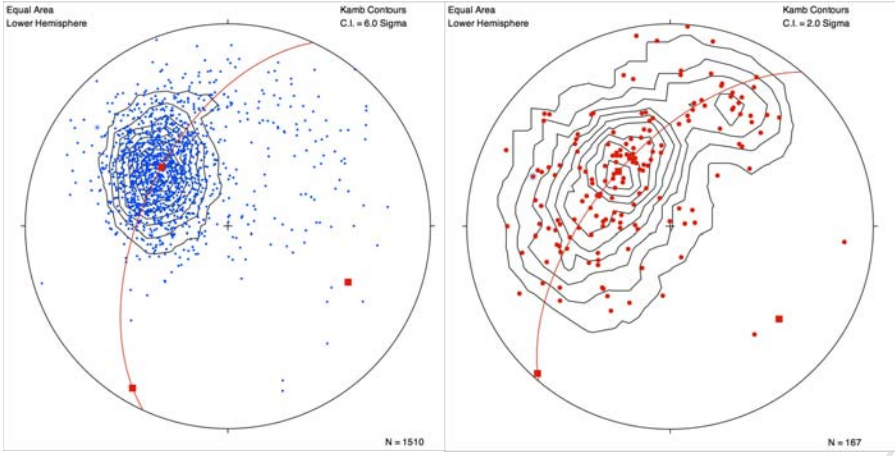

Structural Controls on gold mineralization on the margin of the Yilgarn craton, Albany–Fraser orogen: The Tropicana Deposit, Western Australia

T. G. Blenkinsop[1,2*] and M. G. Doyle[2]

[1] *Economic Geology Research Unit*
School of Earth and Environmental Science,
James Cook University,
Townsville QLD 4811,
Australia
[2]Present Address:
School of Earth and Ocean Sciences,
Main Building, Park Place,
Cardiff CF10 3AT,
United Kingdom
BlenkinsopT@Cardiff.ac.uk
*Corresponding Author

[2] *AngloGold Ashanti Ltd*
Level 13, St Martins Tower
PO Box Z5046, Perth WA 6831
MDoyle@AngloGoldAshanti.com.au

Key words. Shear zone, Archean, Lode gold, orogen, Albany-Fraser, Tropicana

Abstract

The Tropicana gold deposit is located adjacent to the margin of the Yilgarn craton in the Albany–Fraser orogen, Western Australia. The deposit is hosted in granulite facies quartzo-feldspathic gneisses of the Archean Tropicana Gneiss. Ore bodies comprise biotite-pyrite alteration concentrated in shear zones that formed during NE-SW shortening in the late Archean, and clearly postdate the formation and deformation of high-grade gneiss fabrics (D1 and D2). The orientation of the ore bodies is controlled by the shear zones that are in turn localised by the gneissic banding. Mineralization also involved solution and coeval microfracturing and veining of more competent pegmatitic units. The mineralizing event (D3) was followed by at least two further deformations, which reactivated and overprinted the biotite fabrics with sericite and chlorite, created new shear zones, and affected gold distribution. D5 consisted of dextral shear on ~E-W shear zones, which subdivide the deposit into five major structural domains. The importance of structurally controlled permeability at Tropicana is similar in cratonic lode gold deposits, as is the protracted deformation/fluid flow history. Like Renco mine in Zimbabwe, Tropicana gold deposit was formed by hydrothermal fluid flow peripheral to the craton: economic gold mineralization was clearly post-peak metamorphism.

1. Introduction

Many Archean lode gold deposits have distinctive geological characteristics (e.g. Robert and Brown, 1986; Groves et al., 1998; 2000; Wit and Vanderhor, 1998; Goldfarb et al., 2001) including:

1) Discrete, high grade lodes, commonly with abundant quartz and carbonate veining;
2) Greenschist-amphibolite facies peak metamorphism of the host rocks, which slightly predates alteration and mineralization at similar or lower grade metamorphic conditions;
3) A variety of supracrustal host rocks, although Fe-rich and competent lithologies make especially favourable sites for mineralization;
4) Little mineralization in plutonic rocks;
5) A spatial association with felsic intrusions.

In addition to these general geological characteristics, the ore bodies all have in common strong structural controls, which testify to the essential roles of permeability and fluid flow in creating these hydrothermal ore bodies (e.g. Cox, 1999). The controls can be crudely classified in terms of the hosting structure as breccias, faults and shear zones (e.g. Hodgson, 1989). In well-documented cases there is evidence of reactivation of structures and multiple cycles of deformation and fluid flow (e.g. Poulsen and Robert, 1989; Baker et al., 2010; Davis et al., 2010; Miller et al., 2010; Dirks et al., 2013). Increasingly these patterns are interpreted in terms of stress and fluid pressure fluctuations associated with the earthquake cycles (Sibson et al., 1987, 1988; Robert et al., 1995; Cox and Ruming, 2004; Micklethwaite and Cox, 2004; 2006).

At a scale greater than individual deposits, it is well recognised that Archean lode gold deposits are not found directly on craton-scale shear zones, but instead lie in adjacent lower order structures (e.g. Kerrich, 1989; Vearncombe, 1998), although a role for the first order features can be inferred from the distribution of mining camps along them (e.g. Weinberg et al., 2004; Blewett et al., 2010a,b). At a global scale, the occurrence of gold provinces that contain giant or several world class gold deposits has been explained as the consequence of their formation in orogenies involving thin lithosphere or subducted oceanic crust (Bierlien et al., 2001; 2006) because of the greater likelihood of high asthenospheric heat input.

This study describes the structural controls on Australia's largest new gold discovery, the world class Tropicana deposit in Western Australia. The Tropicana deposit is located adjacent to the edge of the Archean Yilgarn craton in the Albany–Fraser orogen (Fig. 1), naturally leading to comparisons with the Archean lode gold deposits of the Yilgarn craton, and posing the question of whether it has formed in a similar way. The aims of this paper are to describe the structural controls on mineralization at Tropicana, to make a comparison with the classic deposits of the Yilgarn craton, and to highlight some remarkable comparisons between the deposit and the Renco gold mine in Zimbabwe. These comparisons cast light on the genesis of the Tropicana deposit.

ACCEPTED MANUSCRIPT

2. Geology of the Tropicana Deposit

2.1 Regional Setting

The Tropicana deposit is situated 41 km to the E of the easternmost magnetic expression of the Archean Yilgarn craton, in the Northern Foreland of the Albany–Fraser orogen (Spaggiari et al., 2011). The proximal part of the Yilgarn craton is the Yamarna Terrane of the Eastern Goldfields Superterrane (Pawley et al., 2012) (Fig. 1). On a regional scale, the boundary between the Northern Foreland and the craton has been interpreted as a major regional structure, the Cundeelee fault, which may have originated as a thrust (Spaggiari et al. 2011). Immediately to the W of the Northern Foreland, a thick sequence of Permo-Carboniferous sedimentary rocks overlies the craton, and is separated from the Northern Foreland around Tropicana by the Gunbarrel fault (Fig. 2), a steeply NW dipping normal fault which cuts the Cundeelee fault. There is no obvious continuity between the NNW trending structures on the Yilgarn craton in the Yamarna terrane (including the Yamarna shear zone) and structures in the Tropicana area of the Northern Foreland (Fig. 2) (e.g. Jones et al., 2006).

The Albany–Fraser orogen mantles the southern and western margins of the Yilgarn craton over a distance of more than 1000 km. Mesoproterozoic orogenic events have been recognised at 1350 – 1260 Ma and 1215-1140 Ma (Clark et al., 2000), but more recently it has become clear that Paleoproterozoic events including deposition of metasedimentary rocks and intrusion of granitic to gabbroic intrusions, constitute a major part of the eastern Albany–Fraser orogeny in the Biranup zone (Kirkland et al., 2011). High grade deformation occurred here at 1680 Ma, called the Zanthus Event within the Biranup orogeny, and this geological history has been interpreted as representing the evolution of an arc-backarc on the margin of the Yilgarn craton (Kirkland et al., 2011).

The Northern Foreland is defined as the reworked part of the Yilgarn craton within the Albany–Fraser orogen (Myers, 1990). The intensity and grade of reworking varies in the Northern Foreland from amphibolite-granulite facies in the S to greenschist-amphibolite facies in the N (Spaggiari et al., 2011). Around and approximately 200 km to the SW of Tropicana, the Northern Foreland consists of a fault-bound assemblage of rocks with a common and distinct geological history that we define as the Plumridge terrane. The Plumridge terrane is approximately 27 km wide at Tropicana: to the E lies the Biranup Zone, consisting of intensely deformed gneiss and metagabbro with Paleoproterozoic ages (Bunting et al., 1976; Spaggiari et al., 2011). The contact between the two zones has a curved NE trending shape in map view, which is overall convex to the NW: it is interpreted as a thrust, herein referred to as the Black Dragon Thrust (Fig. 2). The Black Dragon Thrust juxtaposes ca. 1820 Ma metagranite and amphibolite rocks in the Black Dragon Domain of the Biranup Zone above Archean gneissic rocks hosting the Tropicana deposit, herein referred to as the Tropicana Gneiss (Fig. 2). Deformation in the Biranup zone is associated with the Biranup orogeny (1710 – 1650 Ma), but there was also activity along the Yilgarn margin at 1800 Ma, as indicated by the deposition of sedimentary rocks and intrusion of granites of this age (Spaggiari et al., 2011).

2.2 Host rocks

Neither the host rocks nor the ore body are exposed at Tropicana, being covered by up to 15 m of Cretaceous to Recent sediments. All the data in this study are based on the diamond drilling carried out to delineate the mineral resource. Core was examined from 36 drillholes (Supplementary Material gives drillhole locations), but this did not include any drillholes into the Boston Shaker or the Havana Deeps domains.

The host rocks at Tropicana are gneisses dominated by garnet gneiss (plagioclase, amphibole, garnet ± leucoxene, quartz) and quartzofeldspathic gneiss (plagioclase, k-feldspar, quartz, biotite), with lesser amounts of amphibolite, meta-ferruginous chert (quartz, grunerite), pegmatite and mafic granulite. The pegmatites appear to be products of in situ partial melting at peak metamorphism, which was at upper amphibolite to lower granulite facies (Doyle et al., 2007; 2009). Compositional banding in the gneisses dips moderately to the E to SE (Fig. 4). The hangingwall of the deposit is dominated by the garnet gneiss. The gneisses and the ore bodies are cut by mafic dykes ascribed to the c. 1210 Ma Gnowangerup-Fraser Dyke Suite (Doyle et al., 2007), which are prominent regional aeromagnetic features trending NE (Fig. 2).

2.3 Geochronology

The age of the host rocks regionally was inferred to be Archean (Bunting et al., 1976). This possibility has been strengthened by unpublished propriety geochronological data (Doyle et al., 2009) and preliminary U-Pb zircon ages of

2722± 15 Ma and 2643 ± 7 ma for a metagranite sample taken 7 km N of Tropicana, which have been interpreted as ages of crystallization and metamorphism respectively (Spaggiari et al., 2011).

The retrograde path from peak granulite facies metamorphism is constrained by a rutile U-Pb date of 2524 ± 8 Ma, interpreted to reflect cooling through 500-550°C (Doyle et al., 2013). A minimum age of 2515 ± 8 Ma for mineralization is suggested by biotite Ar-Ar analyses, which is consistent with late Archean Re-Os analyses of pyrite (Doyle et al., 2013). Discordance in zircons and monazites can be interpreted in terms of Pb loss in Stage II of the Albany–Fraser Orogeny (1215-1140 Ma: Kirkland et al., 2011).

3. Ore Geometry and Style of Mineralization

The resource at Tropicana occurs along a 5 km strike length trending overall NE, which can be divided into five structural domains from N to S: Boston Shaker, Tropicana, Havana, Havana Deeps and Havana South (Fig. 3). Low grade mineralization is also recorded to the S of these main areas, for example at Crouching Tiger prospect, and at other prospects regionally (Fig. 2). The five domains have en echelon arrangement. Within each domain the general mineralization envelope trends N to NE. The domains are separated by E to SE trending shear zones, such as the Boston Shaker shear zone between the Boston Shaker and Tropicana domains, and the Swizzler, Cobbler and Don Lino shear zones (Fig. 3). Most of these shear zones dip S. Map scale shears with a similar orientation also occur within the resource areas, as well in a NE direction (Fig. 3).

Mineralization is concentrated in one to several sub-parallel tabular ore zones 2 – 50 m thick which generally dip to the E to SE, within quartzofeldspathic gneiss (Fig. 4). Within these ore zones there are higher grade lenses. When viewed in section parallel to strike, ore zones show an inosculating pattern, separating lenses of unmineralised rock, and thickening and thinning (Fig. 5). The map view of the gold assay data x thickness (gram-metres) shows high grade ore shoots with slightly variable orientations between the domains. In Boston Shaker, the trend is SE, in the northern part of Tropicana, ESE; in Havana and Havana Deeps, SSE (Fig. 3).

Similar distinctions in orientations between the domains are seen in three-dimensional data by examining the orientations of modelled high grade lenses (≥3 g/t) (Fig. 6). Tropicana is characterized by E to SE dipping ore bodies, generally coaxial about an E-plunging line (29° → 087°), whereas the ore bodies in Havana North dip between S and E, and have a common axis plunging to the SSE (22° → 163°).

Gold grades in the ore zones at Tropicana are dominantly associated with intervals of biotite-pyrite alteration that occur within quartzofeldspathic gneiss with pegmatites. Biotite with pyrite and gold replaces metamorphic biotite and amphibole, most commonly in millimetre wide shear zones defined by strong fabrics consisting of elongate biotite and pyrite grains (Fig. 7a,b), but also in disseminated volumes. Higher gold grades are also associated with areas of brecciation in pegmatites around shears, with shears containing biotite-sericite and minor chlorite (Fig. 7c, d), and in areas with solution fabrics (see below; Fig. 8). Known occurrences of visible gold correspond with intercepts of >30 g/t in 1m composite assays. Visible gold is paragenetically late and typically localized on muscovite fractures which cut across anatectic segregations, quartz veins and gneissic bands and biotite-pyrite fracture fills.

4. Deformation History, Meso- and Microstructures

Table 1 gives a deformation history that can be inferred from drill core, geophysics and deposit scale geometry. This section focuses on the detailed evidence from the core pertaining to events which may be associated with gold mineralization: the preceding history is outlined because it affects the deposit geometry.

4.1 Gneissic Banding S1, F1 folds

The most commonly observed mesoscale structure in the cores is a gneissic banding defined by variations of up to 20% in the proportions of quartz, feldspars, biotite, amphibole and garnet on a mm to cm scale (Fig. 9a,b). The gneissic banding is tight to isoclinally folded (Fig. 9a,b) with E to SE dipping hinge surfaces and gently S plunging hinges (Fig. 10). Some of these folds are rootless (Fig. 9b), suggesting that the gneissic banding is the product of early deformation and high grade metamorphism, as indicated by leucosomes that are generally parallel to the banding.

4.2 D2

A fold on the scale of hundreds of m is suggested by W-dipping gneissic banding in cores to the W of the deposit. The drill core data imply an asymmetric synform in the footwall of the mineralization. Based on evidence from the nearest outcrop at Hat Trick Hill (Fox-Wallace, 2010) and regional considerations (Spaggiari et al., 2011), this W verging fold is likely associated with a W to NW verging thrust system that is developed regionally. It is possible that some of the S plunging folds shown in Fig. 10 are F2 folds.

4.2 D3: Shear Zones

Quite distinct from the gneissic banding are localised zones of strong foliation defined by biotite and pyrite, chlorite or sericite (Fig. 7b). Such shear zones are typically mm to cm wide, and clearly cut across the gneissic banding in places, although they are generally parallel to the banding. Asymmetric fabrics indicating shear are common in such zones, and include SC and SC' fabrics, sigma porphyroclasts and oblique foliations (Fig. 9d). Lineations are very difficult to observe because the foliation surfaces are not generally visible in the core. The shear zones are commonly surrounded by zones of brecciation.

Shear zones containing biotite – pyrite only are distinct from those that may also include chlorite or sericite: these minerals appear to overprint the biotite, so that the shear zones containing biotite-pyrite are regarded as a third deformation (D3), after the formation and folding of the gneissic fabric, but predating later overprinting by other phyllosilicates.

4.3 D3: Solution Fabrics and Breccias

Zones of intense solution fabrics are defined by wavy seams containing biotite and pyrite 1 – 2 mm wide between fractured quartz and feldspar layers 5 – 10 mm thick (Fig. 8). In places the fracturing is dense enough to be described as a breccia (Fig. 8b). The quartz and feldspar are fractured by mm long veins filled with calcite that form distinctive irregular shapes perpendicular to the stylolites (Fig. 8a). The calcite veins appear to be extensional and in places are markedly oblique to the solution seams. They are associated with ostensibly the same auriferous pyrite as the solution seams, since that pyrite can be seen as a component of the fracture fill in the carbonate veins (Fig. 8d), and biotite alteration in the seams extends into the fractures. The presence of biotite and pyrite suggests that this fabric may have formed during D3, although there is also a strong association with sericite in places. Significant gold grades were recovered from a stylolitic interval in core from drill hole TP202.

4.4 D3 Folds

Gentle folds of the lithological layering visible in the mine model plunge moderately SE and occur on the scale of whole domains. Folding with a similar orientation can be inferred from the distribution of poles to gneissic banding (Fig. 11), and from some measurements of individual folds in core (Fig. 10). This folding postdates D1 and D2, and is ascribed to D3.

4.3 D4, D5 Shear Zones and Folds

Some biotite-pyrite shear zones are overprinted by fabrics defined by chlorite and sericite, which have distinct kinematics. Other shear zones contain sericite and chlorite only. A distinctive set of shear zones with biotite and sericite/chlorite dip S and SW and have dextral kinematics. Some of these later fabrics are folded into characteristically asymmetric folds on a 1 - 10 cm scale (Fig. 9c). These folds have been measured at the boundary between the Tropicana and Havana domains, near the Boston Shaker shear zone. Fold hinge surfaces dip S, with generally E to SE plunging hinges (Fig. 10) and Z asymmetries. The folds and the S dipping dextral shears are consistent with a late deformation event comprising dextral shear on S and SW dipping zones. Since they fold a sericite-chlorite fabric, this event (D5) probably postdates an intermediate event represented by sericite-chlorite shear zones in various orientations (D4).

5. Kinematic Analysis

Shear zones were measured from cores into the Tropicana, Havana North and South domains (Fig. 12). Kinematic analysis of shear zones was possible from SC and SC' fabrics and sigma clasts which could be used to identify the vorticity vector and hence the shear direction as perpendicular to the vector. A kinematic analysis was performed using linked Bingham axes (cf. Marrett and Allmendinger, 1990) and filtering the results by the phyllosilicate mineralogy of the shear zones into biotite, biotite with sericite and/or chlorite, and sericite/chlorite groups (Figs. 12, 13). In all cases the linked Bingham axes from the kinematic analysis give one of two shortening directions: NE or NW (Fig. 13).

The biotite shear zones dip to the SW, S, SE and NE (Fig. 12). Kinematics vary consistently with orientation: SW, S and SE dipping shears are sinistral, while E and NE dipping shears are dextral (Fig. 12). The displacement pattern is kinematically coherent, and consistent with NE horizontal shortening, which is also reflected by the linked Bingham axes (Fig. 13). This orientation defines D4 kinematics.

The other shear zones have similar orientations to the biotite shears, but in all orientations there is a variety of shear directions and senses (Figs. 12, 13), commonly with contradictory shear senses on adjacent and sub-parallel shears. A particularly common set of shears dips S to SW with mostly dextral normal kinematics: these are common at the major breaks between the Tropicana and Havana North domains and between the Havana North and South domains, (e.g. holes TFRC090D and TFD167) (Figs. 11, 12), and they define the D5 kinematics with a NW shortening direction. The same shortening direction is apparent from shears that have sericite/chlorite and no biotite, which can be associated with D5 (Table 1).

Shear zones with biotite and sericite/chlorite show some overlap between shortening and extensional quadrants, and the Bingham axes reflect either NE or NW shortening (Fig. 14). This is consistent with the possibility that some of these shear zones have been reactivated in D5 kinematics, while others preserve D3 shortening directions.

6. Discussion

6.1 Deformation History and Structural Controls on Ore bodies at Tropicana

The structural/mineralization history at Tropicana is summarised in the cartoons of Fig. 16. D1 included the formation of high-grade gneissic banding, partial melting, and isoclinal folding (Fig. 16a). The kinematics of D1 could not be constrained by observations in this study, and the event as defined here might include additional complexities. Regional considerations suggest that D2 was a major event of W to NW directed thrusting that probably created some of the major structures in the area such as the Iceberg thrust (Fig. 16b). Tight to isoclinal folds in gneissic banding plunging S to SE observed in the core cannot definitively be ascribed to D1 or D2, and it is possible that they represent a progressive deformation event.

Gold mineralization at Tropicana is controlled by a system of biotite-pyrite shear zones within a favourable lithological band of feldspathic gneiss that has a sheet dip to the E to SE. The biotite shear zones are generally sub-parallel to gneissic banding, but clearly postdate it, and are surrounded by diffuse bodies of mineralised breccia. The main mineralization phase was associated with the biotite alteration, and the shear zones formed with a NE shortening direction (Fig. 14).

The biotite-pyrite shear zones measured in the core have an approximate girdle distribution around a SE-trending axis (Fig. 15). Although the shears have a variety of orientations, they are not folded on the scale of the core. The SE trend is similar to the direction of the high grade ore shoots visible on the map (Fig. 3) and to the common intersection of high-grade ore shells in Havana (Fig. 6). Gentle folding of the gneissic banding in this orientation is also apparent on a large scale (Fig. 11): these are ascribed to an F3 generation of folds.

The SE trend observed in the gram-metre plot, the high grade ore shells, the girdle distribution of the shears and the orientations of gneissic banding, is a very significant control on mineralization, which is consistent with fluid flow along the biotite-pyrite shears. The observation that the biotite-pyrite shears are not folded and the similarity of Figs. 11 and 15 suggest that their orientation was largely controlled by the gneissic banding, to which they are generally parallel. The orientation of the gneissic banding reflects D1 and D2, which imparted the moderate E to SE dip to the banding, and a component of gentle folding superimposed in D3. The trends of the high grade shoots are therefore parallel to common intersections of the biotite-pyrite shear zones and hinges of F3 folds (Fig. 16c).

There are significant variations in these trends between Tropicana and the other domains. In Tropicana, high grade ore shells dip more easterly than in Havana (Fig. 6), giving an easterly trend to their intersection, which is also apparent in the gram-metre plot (Fig. 3). At least two possibilities to explain this variation are: i) an initial variation in geometry inherited from D1 and D2; or ii) Reorientation by D4 or D5 in Tropicana, which is distinguished from the other domains by a higher density of late shear zones.

Lower grade sericite/chlorite fabrics overprint the biotite-pyrite shears. SC and SC' fabrics were developed during this retrogression. The distinct group of S to SW dipping shear zones observed in the cores with sericite/chlorite and dominantly dextral normal kinematics near the junction of boundaries of the structural domains

(Fig. 12) have a NW shortening direction, and define the D5 kinematics (Fig 16d). The distinctive Z folds near the Boston Shaker shear zone are consistent with D5.

Notwithstanding the general history given above, there are examples of contradictory shear senses, some even within the mineralising biotite-pyrite shears. These testify to repeated reactivation, commonly in opposite shear senses, which is a hallmark of the deposit. Much of the reactivation is consistent with D5 overprinting D3 structures, but there are anomalous shear zones that do not fit in with this history: they could represent the influence of D4. However, the kinematics of D3 and D5 appear to be dominant (Fig. 14).

N trending shears observed in some cores (Fig. 12) are parallel to a change in structural grain observed on a large scale around Tropicana and in the Plumridge terrane compared to other parts of the Northern Foreland, where aeromagnetic trends are NW and more comparable with adjacent trends in the Yamarna Terrane. This inflexion may have been important to mineralization by bringing lithological bands into a more favourable orientation for shearing.

6.2 Comparison with Archean lode gold deposits

In terms of its general geological properties, the Tropicana deposit has some similarities but also significant differences from many Archean lode gold deposits of the Yilgarn craton. Tropicana lacks the metre scale quartz carbonate veining that is such a characteristic feature of many Archean lode gold deposits.

Likewise, the upper amphibolite-granulite grade of metamorphism for the host rocks is exceptional, while the occurrence of mineralization at greenschist facies at Tropicana (Doyle et al., 2009) is more typical of lode gold deposits (e.g. Vearncombe, 1998). The concentration of mineralization in the feldspathic gneiss is comparable to preferential mineralization in some host rocks within lode gold deposits, although the feldspathic gneiss itself is quite dissimilar geochemically to the basaltic or andesitic volcanic hosts of many lode gold deposits. The diffuse nature of many ore bodies at Tropicana, which occur in volumes of altered rock that do not have discrete structural boundaries, is also atypical of lode gold deposits, in which ore bodies are commonly confined by vein, fracture, fault or shear margins.

However, the structural control by shear zones at Tropicana is similar to some lode gold deposits, as is the role of solution and brecciation (e.g. Witt and Vanderhor, 1998). Shear zones at Tropicana exist in many orientations (Fig. 12): similarly orientated shear zones can have quite different kinematics (Fig. 13). This feature is also typical of some lode gold deposits (see below) in which, as at Tropicana, it is probably due to overprinting events, several of which may be associated with gold mineralization and remobilization. The main phase of economic gold mineralization at Tropicana is Archean and postdates D1 and D2 deformation events: in this respect it is also similar to Archean lode gold deposits of the Yilgarn craton, although the timing of mineralization at Tropicana does not appear to correspond with the majority of late Archean deposits on the craton. Nevertheless, Tropicana fits well into the suggested categorization of those deposits as “late orogenic, structurally controlled” (Witt and Vanderhor, 1998).

It is difficult to establish how much new mineralization as opposed to remobilisation may have been associated with D4 and D5 at Tropicana. Remobilisation of gold is evidenced by clusters of visible gold localised in late muscovite fabrics that overprint earlier biotite-pyrite fracture fills and grains. Several detailed studies of large lode gold deposits show that they have experienced more than one mineralizing event (e.g. the Golden Mile; Vielreicher et al., 2010) or that reactivation has been a significant part of the deposit history (e.g. St Ives: Miller et al., 2010; Renco Mine, Kolb and Meyer, 2002; Sunrise Dam: Baker et al., 2010). The evidence for reactivation at Tropicana is a point of comparison with the Archean lode gold deposits.

The timing of D3 and the main mineralizing event (Tropicana event) is well constrained to the late Archean by Ar-Ar dating of biotite and Re-Os dating of pyrite (Doyle et al., 2013). From a regional perspective there are at least three possibilities for the reactivation recorded by D4 and D5 at Tropicana. The Zanthus event of the Biranup orogeny occurred at c. 1680 Ma, and the two stages of the Albany–Fraser orogeny occurred at 1345–1260 Ma (Stage I) and 1215–1140 Ma (Stage II) (Kirkland et al., 2011). The Eastern Biranup zone, in contact with the Northern Foreland to the E of Tropicana, has no geochronological evidence for Stage I of the Albany–Fraser orogeny (Kirkland et al., 2011), which is consistent with a lack of evidence for this event in zircon or monazite. However, low grade deformation and fluid flow related to this event can not be excluded. Thrust emplacement of the Eastern Biranup Zone over the Northern Foreland is likely to have occurred in the later stage of the Albany–Fraser orogeny, which most probably correlates with the clearest evidence of reactivation at Tropicana, in D5.

6.3 Comparison with Renco Deposit, Zimbabwe

Renco gold mine in Zimbabwe is in a granulite terrane (the Northern Marginal Zone) 10 km from the contact between the granulites and the Zimbabwe Archean craton. The mine is hosted by a late Archean enderbite intrusion (Blenkinsop et al., 2004). The mineralization lies in shear zones that dip moderately away from the craton, and in steeper linking shear zones (Kisters et al., 1998). Mineralization probably occurred in upper amphibolite facies conditions at the end of the Archean (Kolb et al., 2000), although evidence for a lower grade of mineralization suggests that there was a second, possibly Paleoproterozoic event (Frei et al., 1999; Blenkinsop et al., 2004). Reactivation is also evidenced by low grade fabrics in the shear zones (Kolb et al., 2003). Within the shear zones that host the mineralization, two domains are distinguished: quartz-feldspar-biotite-hornblende mylonites, which surround lithons of k-feldspar-quartz-biotite-garnet-sulphide. Fractures in lithons are filled by sulphides, and the majority of the grade is concentrated in them (Kisters et al., 2000).

The similarity in the position of Renco and Tropicana as gold deposits in granulite terranes relative to their adjacent cratons is striking, and this is reinforced by the common geometry of the ore bodies in zones that dip moderately away from the craton. A network of shear zones is the critical hydrogeological structure in both cases, and the fractured lithons of Renco have their counterpart in the brecciated pegmatite bodies of the Tropicana deposit. Both deposits also have evidence for lower metamorphic grade overprints on granulite facies host rocks.

The timing of Renco mineralization is considered to be post-peak granulite facies metamorphism in the late Archean, on a retrograde path but within 100°C of peak metamorphism (Kolb and Meyer, 2002). The post-peak conditions and timing are another similarity to Tropicana. The timing and geology of these deposits suggest a possible link to granulite facies metamorphism in as much as the deposits can be interpreted as forming in the retrograde parts of an orogenic cycle that reached peak granulite facies. However, Kerrich (1988) has shown that there is unlikely to be a direct geochemical link between granulite formation and lode gold deposits: additional fluid input is probably required to explain characteristic Large Ion Lithophile (LILE) enrichment of alteration associated with mineralization compared to the depleted LILE characteristics of Archean granulites.

7. Conclusions

Tropicana gold deposit in the Albany Fraser orogen on the margin of the Yilgarn craton was formed by fluid flow through a network of biotite-pyrite-bearing shear zones, initially in an event of NE shortening (D3). Permeability was created in coarser, more competent pegmatitic layers by fracturing, and was accompanied by solution transfer along solution seams. Shear zones were reactivated to provide a record of complex kinematics, including two retrograde events (D4 and D5). D5 involved dextral shear on S-SW dipping surfaces.

The most important geometrical control on mineralization at Tropicana is the permeability created by the biotite-pyrite-bearing shear zones. The orientation and location of these in turn were largely dictated by the orientation of the gneissic banding in the favourable horizon of host rocks, which reflects two previous deformation events and gentle folding in D3. High grade ore shoots formed parallel to the common intersection direction of the shear zones, which was also parallel to F3 fold hinges. Variations in the direction of the ore shoots could reflect variations in the initial geometry of the gneisses, and/or later deformation. A consideration of the entire geological history is necessary to understand the deposit geometry.

The style of mineralization at Tropicana is different from many Archean lode gold deposits of the Yilgarn craton in as much as no metre scale quartz/carbonate veins, fractures or faults seem to have played an important role in mineralization. Nevertheless, the Tropicana deposit has a strong structural control, in common with the Archean lode gold deposits, because all these deposits were formed by hydrothermal fluid flow along structural permeability. Mineralization at Tropicana occurred at greenschist facies in granulite facies host rocks, clearly post-dating peak metamorphism.

Renco mine in Zimbabwe and Tropicana gold deposit have several characteristics in common, including their formation within granulites at the margins of well-mineralized Archean cratons, probably within the late Archean. It is possible that both could have been formed by fluid flow driven by heat sources reflecting the waning of granulite facies metamorphism in orogenic belts on the periphery of their respective Archean cratons.

Acknowledgements

Independence Group NL and AngloGold Ashanti Ltd are thanked for permission to publish the manuscript. The authors acknowledge the significant contribution of past and present AngloGold Ashanti geologists and the exploration team who have contributed to the discovery, delineation and understanding of the mineral deposit. In particular, we are grateful for the assistance of Jeni Savage and Jovo Przulj in completing the study.

References

Baker, T., Bertelli, M., Blenkinsop, T., 2010. PTX conditions of fluids in the Sunrise Dam gold deposit, Western Australia, and implications for the interplay between deformation and fluids. Economic Geology 105, 873–894.

Bierlein, F.P., Hughes, M., Dunphy, J., McKnight, S., Reynolds, P.R., Waldron, H., 2001. Tectonic and economic implications of trace element, 40Ar/39Ar and Sm–Nd data from mafic dykes associated with orogenic gold mineralisation in central Victoria, Australia. Lithos 58, 1–31.

Bierlein, F.P., Groves, D.I., Goldfarb, R.J., Dubé, B., 2006. Lithospheric controls on the formation of provinces hosting giant orogenic gold deposits. Mineralium Deposita 40, 874–886.

Blenkinsop, T.G., 2006. Fluid flow in shear zones: insights from the geometry and evolution of ore bodies at Renco gold mine, Zimbabwe. Geofluids 6, 334-345.

Blenkinsop, T.G., Doyle, M.G., 2010. A method for measuring the orientations of planar structures in cut core. Journal of Structural Geology 32, 741–745.

Blenkinsop, T. G., 2011. Archean magmatic granulites, diapirism, and Proterozoic reworking in the Northern Marginal Zone of the Limpopo Belt. Geological Society of America Memoir 207, 245-267.

Blenkinsop, T.G., Kröner, A., Chiwara, V., 2004. Single stage , late Archaean exhumation of granulites in the Northern Marginal Zone , Limpopo Belt , Zimbabwe , and relevance to gold mineralization at Renco mine. South African Journal of Geology 107, 377–396.

Blewett, R.S., Czarnota, K., Henson, P.A., 2010a. Structural-event framework for the eastern Yilgarn Craton, Western Australia, and its implications for orogenic gold. Precambrian Research 183, 203–229.

Blewett, R.S., Henson, P.A., Roy, I.G., Champion, D.C., Cassidy, K.F., 2010b. Scale-integrated architecture of a world-class gold mineral system: The Archaean eastern Yilgarn Craton, Western Australia. Precambrian Research 183, 230–250.

Bunting, J.A., De Laeter, J.R., Libby, W.G., 1976. Tectonic subdivisions and geochronology of the northeastern part of the Albany–Fraser Province, Western Australia, in Annual report for the year 1975: Geological Survey of Western Australia, Perth, Western Australia, p. 117–126.

Cameron, E., 1988. Archean gold: Relation to granulite formation and redox zoning in the crust. Geology 16, 1–4.

Clark, D.J., Hensen, B.J., Kinny, P.D., 2000. Geochronological constraints for a two-stage history of the Albany–Fraser Orogen, Western Australia: Precambrian Research, v. 102, no. 3, p. 155–183.

Cox, S.F., 1999. Deformational controls on the dynamics of fluid flow in mesothermal gold systems. Geological Society, London, Special Publications 155, 123–140.

Cox, S.F., Ruming, K., 2004. The St Ives mesothermal gold system, Western Australia—a case of golden aftershocks? J. Struct. Geol. 26 (2004) 1109–1125.

Davis, B.K., Blewett, R.S., Squire, R., Champion, D.C., Henson, P. A., 2010. Granite-cored domes and gold mineralisation: Architectural and geodynamic controls around the Archaean Scotia-Kanowna Dome, Kalgoorlie Terrane, Western Australia. Precambrian Research 183, 316–337.

Dirks, P.H.G.M., Charlesworth, E.G., Munyai, M.R., Wormald, R., 2013. Stress analysis, post-orogenic extension and 3.01Ga gold mineralisation in the Barberton Greenstone Belt, South Africa. Precambrian Research 226, 157–184.

Doyle, M.G., Kendall, B.M., Gibbs, D., 2007. Discovery and characteristics of the Tropicana Gold District. In: Bierlein F.P., and Knox-Robinson C.M. (editors), 2007. Proceedings of Geoconferences, Kalgoorlie 07 Conference, Geoscience Australia Record 2007/14, pp.186–190.

Doyle M.G., Gibbs, D., Savage J., , Blenkinsop, T.G., 2009. Geology of the Tropicana Gold Project, Western Australia. In: In Williams P.J., et al. (editor) Smart science for exploration and mining; Proceedings of the tenth biennial SGA meeting, Townsville, p.50–52.

Doyle, M. G., Savage, J., Blenkinsop, T.G., Crawford, A., McNaughton, N. 2013 Tropicana: Unravelling a +6Moz Gold Deposit Hosted in Granulite Facies Metamorphic Rocks. The Australian Institute of Mining and Metallurgy Publication Series 9/2013, 87–93.

Fox-Wallace L.J., 2010. Geology of the Hat Trick Prospect in the Tropicana Project area, Western Australia. Unpublished Bsc. (Hons.) thesis, James Cook University, p. 104.

Frei, R., Blenkinsop, T.G., Schonberg, R., 1999. Geochronology of the late Archaean Razi and Chilimanzi suites of granites in Zimbabwe: implications for the late Archaean tectonics of the Limpopo Belt and Zimbabwe Craton South African Journal of Geology 102, 55–64.

Goldfarb, R.J., Groves, D.I., Gardoll, S., 2001. Orogenic gold and geologic time: a global synthesis. Ore Geology Reviews 18, 1–75.

Groves, D.I., Goldfarb, R.J., Gebre-Mariam, M., Hagemann, S.G., Robert, F., 1998. Orogenic gold deposits: A proposed classification in the context of their crustal distribution and relationship to other gold deposit types. Ore Geology Reviews 13, 7–27.

Groves, D.I., Goldfarb, R.J., Knox-Robinson, C.M., Ojala, J., Gardoll, S., Yun, G.Y., Holyland, P., 2000. Late-kinematic timing of orogenic gold deposits and significance for computer-based exploration techniques with emphasis on the Yilgarn Block, Western Australia. Ore Geology Reviews 17, 1–38.

Hodgson, C.J., 1989. Patterns of Mineralization, in: Bursnall, J.T. (Ed.), Mineralization and Shear Zones: Short Course Notes Volume 6. Montreal, pp. 51–88.

Kerrich, R., 1988. Archean gold□: Relation to granulite formation or felsic intrusions□? Geology 17, 1011–1015.

Kerrich, R., 1989. Geodynamic setting and hydraulic regimes: shear zone hosted mesothermal gold deposits, in: Bursnall, J. (Ed.), Mineralization and Shear Zones: Geological Association of Canada Short Course Notes 6. Montreal, pp. 89–128.

Kirkland, C.L., Spaggiari, C.V., Pawley, M.J., Wingate, M.T.D., Smithies, R.H., Howard, H.M., Tyler, I.M., Belousova, E.A., Poujol, M., 2011. On the edge: U–Pb, Lu–Hf, and Sm–Nd data suggests reworking of the Yilgarn craton margin during formation of the Albany–Fraser Orogen. Precambrian Research 187, 223–247.

Kisters, A. F. M., Kolb, J., Meyer, F.M., 1998. Gold mineralizaation in high-grade metamorphic shear zones of the Renco Mine, southern Zimbabwe. Economic Geology 93, 587–601.

Kisters, A.F.M., Kolb, J., Meyer, F.M., Hoernes, S., 2000. Hydrologic segmentation of high-temperature shear zones: structural, geochemical and isotopic evidence from auriferous mylonites of the Renco mine, Zimbabwe. Journal of Structural Geology 22, 811–829.

Kolb, J., Kisters, A., Hoernes, S., Meyer, F., 2000. The origin of fluids and nature of fluid–rock interaction in mid-crustal auriferous mylonites of the Renco mine, southern Zimbabwe. Mineralium Deposita 35, 109–125.

Kolb, J., Kisters, A.F.M., Meyer, F.M., Siemes, H., 2003. Polyphase deformation of mylonites from the Renco gold mine (Zimbabwe): identified by crystallographic preferred orientation of quartz. Journal of Structural Geology 25, 253–262.

Kolb, J., Meyer, M.F., 2002. Fluid inclusion record of the hypozonal orogenic Renco gold deposit (Zimbabwe) during the retrograde P–T evolution. Contributions to Mineralogy and Petrology 143, 495–509.

Marrett, R., Allmendinger, R.W., 1990. Kinematic analysis of fault-slip data. Journal of Structural Geology 12, 973–986.

Micklethwaite, S., Cox, S.F., 2004. Fault-segment rupture, aftershock-zone fluid flow, and mineralization. Geology 32, 813.

Micklethwaite, S., Cox, S., 2006. Progressive fault triggering and fluid flow in aftershock domains: Examples from mineralized Archaean fault systems. Earth and Planetary Science Letters 250, 318–330.

Miller, J., Blewett, R., Tunjic, J., Connors, K., 2010. The role of early formed structures on the development of the world class St Ives Goldfield, Yilgarn, WA. Precambrian Research 183, 292–315.

Myers J.S., 1990. Albany–Fraser Orogen. In Geology and mineral resources of Western Australia: Western Australia Geological Survey, Memoir 3, p. 255–264.

Pawley, M.J., Wingate, M.T.D., Kirkland, C.L., Wyche, S., Hall, C.E., Romano, S.S., Doublier, M.P., 2012. Adding pieces to the puzzle: episodic crustal growth and a new terrane in the northeast Yilgarn Craton , Western Australia. Western Australia. Australian Journal of Earth Sciences 59, 603–623.

Poulsen, H., Robert, F., 1989. Shear zones and gold: Practical examples from the southern Canadian Shield, in: Bursnall, J.T. (Ed.), Mineralization and Shear Zones, Geological Association of Canada, Short Course Notes 6. Montreal, pp. 239–266.

Robert, F., Brown, A.C., 1986. Archean gold-bearing quartz veins at the Sigma mine, Abitibi greenstone belt, Quebec. Part I. Geologic relations and formation of the vein systems. Economic Geology 81, 578–592.

Robert, F., Boullier, A.-M., Firdaous, K., 1995. Gold-quartz veins in metamorphic terranes and their bearing on the role of fluids in faulting. Journal of Geophysical Research: Solid Earth 100, 12861–12879.

Sibson, R., 1987. Earthquake rupturing as a mineralizing agent in hydrothermal systems. Geology 15, 710–704.

Sibson, R., Robert, F., Poulsen, K., 1988. High-angle reverse faults, fluid-pressure cycling, and mesothermal gold-quartz deposits. Geology 16, 551-555.

Spaggiari C.V., Kirkland C.L., Pawley M.J., Smithies R.H., Wingate M.T.D., Doyle M.G., Blenkinsop T.G., Clarke C., Oorschot L.J., Fox, L.J., Savage J., 2011. The geology of the East Albany-Fraser Orogen – A field guide. Geological Survey of Western Australia, Record 2011/23, 98p.

Vearncombe, J.R., 1998. Shear zones, fault networks, and Archean gold. Geology 26, 855.

Vielreicher N.M., Groves D.I., Snee L.W., Fletcher I.R., McNaughton N.J., 2010: Broad synchroneity of three gold mineralisation styles in the Kalgoorlie gold field: SHRIMP, U-Pb, and $^{40}Ar/^{39}Ar$ geochronological evidence. Economic Geology 105, pp. 187-227.

Weinberg, R.F., Hodkiewicz, P.F., Groves, D.I., 2004. What controls gold distribution in Archean terranes? Geology 32, 545.

Witt, W.K., Vanderhor, F., 1998. Diversity within a unified model for Archaean gold mineralization in the Yilgarn Craton of Western Australia: An overview of the late-orogenic, structurally-controlled gold deposits, Ore Geology Reviews 13, 29-64,

Figures

Fig. 1. Location of Tropicana gold deposit in the Northern Foreland of the Albany–Fraser orogen (partly based on Spaggiari et al., 2011, Pawley et al., 2012).

Fig 2. Simplified interpretive geological map of the Tropicana region. The Black Dragon thrust separates the Archean Tropicana Gneiss in the Plumridge terrane from lower metamorphic grade rocks of the Paleoproterozoic Biranup zone. Other NNE to NE trending structures separate further subdivisions of the Albany–Fraser orogen.

Fig. 3. Structural domains and mesoscopic shear zones of the Tropicana Deposit, superimposed on a grade (g/t) X thickness (m) plot. GDA/UTM grid.

Fig. 4. Schematic EW cross section of the Tropicana Deposit (based on Doyle et al., 2007).

Fig. 5. NE-SW section (true scale). Blue shapes are delimited by > 3g/t. “Principal lineation” refers to the high grade ore shoots seen in the gm plot of Fig. 3. High grade ore bodies pinch and swell.

Fig. 6. Stereoplots of poles to high grade (>3 g/t) ore shells. A distinct difference is noted between the Tropicana and Havana domains. Red squares are eigenvectors of the distribution of poles. The minimum eigenvector is labelled with its trend and plunge; a great circle connects the minimum and intermediate eigenvectors. All stereoplots are lower hemisphere, equal area.

Fig. 7. Styles of Mineralization in the core.

a) Biotite-pyrite shear zone sub-parallel to gneissic banding, core TPD366, 160 m.

b) Biotite-pyrite shear zone (thin section). Foliation defined by biotite and pyrite gives clear top-to-the left sense of shear. Core TPD361A, 161 m, XPL (Cross-polarised light).

c) Chlorite-sericite shear zone, core TPD167, 163.2 m. Asymmetric clast gives clear shear sense.

d) Sericite shear zone (thin section). Spectacular SC fabrics defined by sericite and pyrite give clear top-to-the-right shear sense. Core TPD067, 143.3 m, XPL.

Fig. 8. Styles of mineralization in the core.

a) Solution seams with biotite anastomosing between feldspar-rich lithons with carbonate-filled extension fractures. TPD202, 281.9 m

b) Fragmentation and solution accompanying formation of carbonate-sericite-pyrite veins. TPD202B, 282.9 m, XPL.

c) More discrete formation of biotite lined solution seams and irregularly-shaped patches of carbonate. TPD 202, 285.8 m

d) Extension microfracture in perthite grain, with filling of pyrite and carbonate. TPD202C, 283.9 m, XPL

Fig. 9. Structural features in core.

a) F1 folds in gneissic banding. Yellow lines marks form surface, yellow spots are hinges and red line is hinge surface trace. TPD251, 222.7 m.

b) Tight F1 fold hinge of gneissic banding, TPD202, 314.1 m.

c) Asymmetric F5 fold of gneissic banding and shear foliation. TPRC092D, 298.7 m.

d) SC' defined by chlorite and sericite. Marking according to the scheme of Blenkinsop and Doyle (2010). TPD262, 162m.

Fig. 10. Orientations of fold hinges and hinge surfaces, located relative to drillholes and structural domains. Folds in cores MBRC019D, TPRC607D, TFD137, TFRC501D, TPD202, TPD261 and TPD366 plunge moderately S to SE with E to SE dipping hinge surfaces. These are interpreted as F1 or F2 folds, because they are tight to isoclinal. Folds in cores TFRC090D and TFRC092D plunge moderately E to SE with S-dipping hinges surfaces. Many of these have dextral vergence (turquoise colour). These folds are located adjacent to the Boston Shaker shear zone and are F5 folds. Alternatively those folds which are symmetric could be F3.

Fig. 11. Poles to gneissic banding (n = 1510) in the Havana domain. Cylindrical best fit gives a fold hinge plunging 35° to 115°. Kamb contours with a contour interval of 6σ, 3σ significance level.

Fig. 12. Geographic distribution of shear zones in ball-and-string plots. Great circles indicate shear planes: arrows indicate hangingwall movement. In most plots there are sub-parallel shears with different movement directions, testifying to reactivation.

Fig. 13. Tangent lineation plots of shear zones separated by structural domain and by phyllosilicate mineralogy. Arrows indicate footwall movement, plotted at the pole to the fault. Dextral components in green and sinistral in red.

Fig. 14. Kinematic analysis of shear zones separated by structural domain and by phyllosilicate mineralogy. Red and blue dots are shortening and lengthening axes for individual shear zones respectively; 1, 2, and 3 are the linked Bingham axes for the distributions shown.

Fig. 15. Poles to shear zone orientations in four structural domains, with eigenvectors to the distributions shown as black squares. Great circle links maximum and intermediate eigenvectors. Kamb contours, Contour interval 2σ, significance level 3σ.

Fig. 16. Cartoon of the structural evolution of the Tropicana Gold Deposit

a) D1 is preserved as asymmetric folds and gneissic banding

b) D2: thrusting (orange surfaces) and folding is inferred from regional considerations

c) D3: the main mineralizing event, due to NE shortening

d) D5: The main reactivation

		D1	D2	D3	D4	D5
	Macro structure		Thrusts Folds	SE plunging folds		Shear zones
	Meso-micro structures	Gneissic Banding Isoclinal folds		Shear zones Solution fabrics Breccias	Shear zones	Shear zones Asymmetric folds
	Kinematics	?	NW shortening	NE Shortening	?	Dextral E-NE shearing
Au:	**Biotite**			———		
High	**Pyrite**			———		
↓	**Sericite**			- - - -	———	———
Low	**Carbonate**			- - - -		
	Chlorite			- - - -		
	Timing	2640-2524	2640-2524	2524-2515	?	? 1215-1140

Table1. Deformation and mineralization history at Tropicana Gold Mine

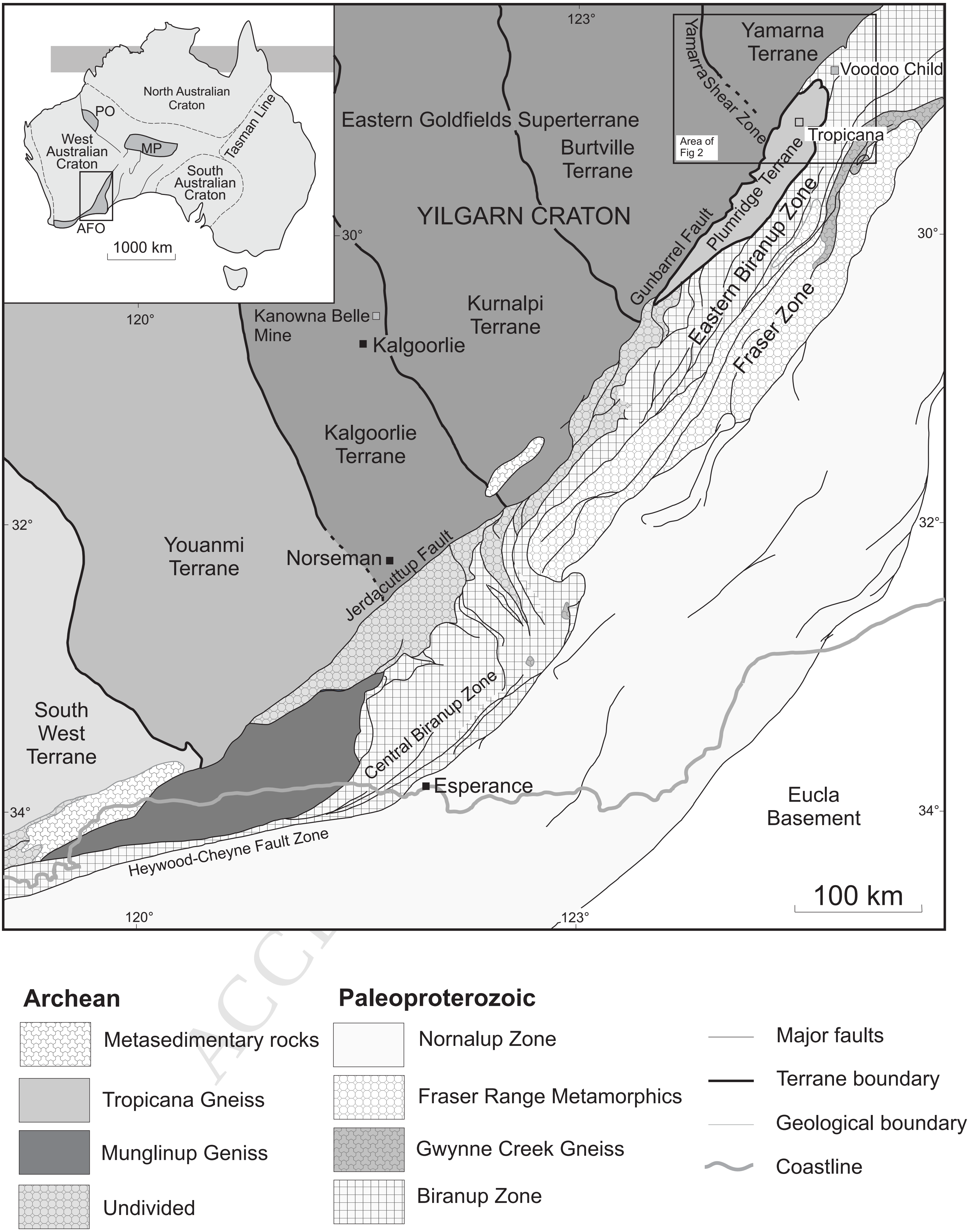

Albany-Fraser bedrock interp.cdr

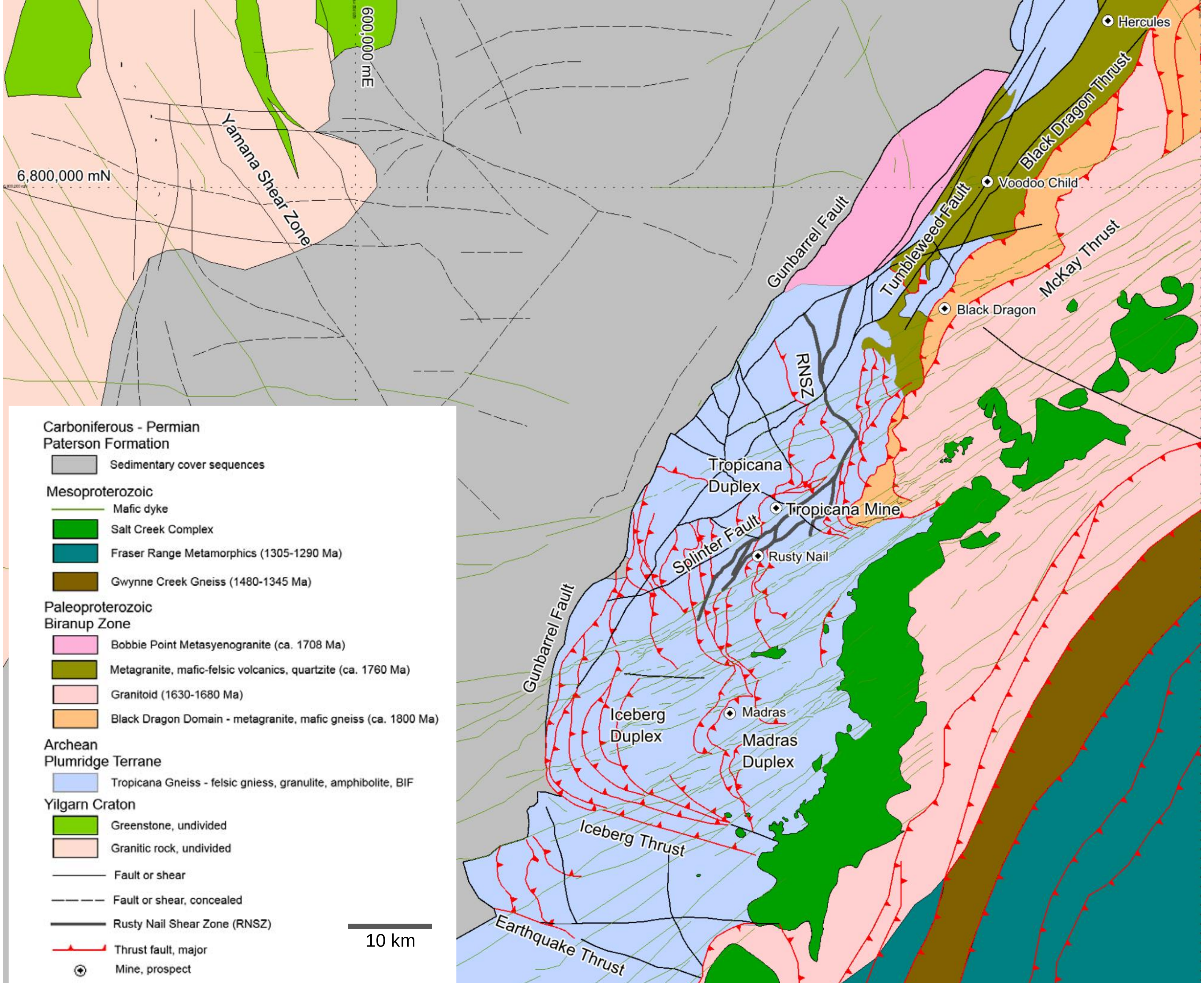

600,000 mE
6,800,000 mN
Yamana Shear Zone
Gunbarrel Fault
Tumbleweed Fault
Black Dragon Thrust
Hercules
Voodoo Child
McKay Thrust
Black Dragon
RNSZ
Tropicana Duplex
Tropicana Mine
Splinter Fault
Rusty Nail
Gunbarrel Fault
Iceberg Duplex
Madras
Madras Duplex
Iceberg Thrust
Earthquake Thrust
10 km
Carboniferous - Permian
Paterson Formation
Sedimentary cover sequences
Mesoproterozoic
Mafic dyke
Salt Creek Complex
Fraser Range Metamorphics (1305-1290 Ma)
Gwynne Creek Gneiss (1480-1345 Ma)
Paleoproterozoic
Biranup Zone
Bobbie Point Metasyenogranite (ca. 1708 Ma)
Metagranite, mafic-felsic volcanics, quartzite (ca. 1760 Ma)
Granitoid (1630-1680 Ma)
Black Dragon Domain - metagranite, mafic gneiss (ca. 1800 Ma)
Archean
Plumridge Terrane
Tropicana Gneiss - felsic gniess, granulite, amphibolite, BIF
Yilgarn Craton
Greenstone, undivided
Granitic rock, undivided
Fault or shear
Fault or shear, concealed
Rusty Nail Shear Zone (RNSZ)
Thrust fault, major
Mine, prospect

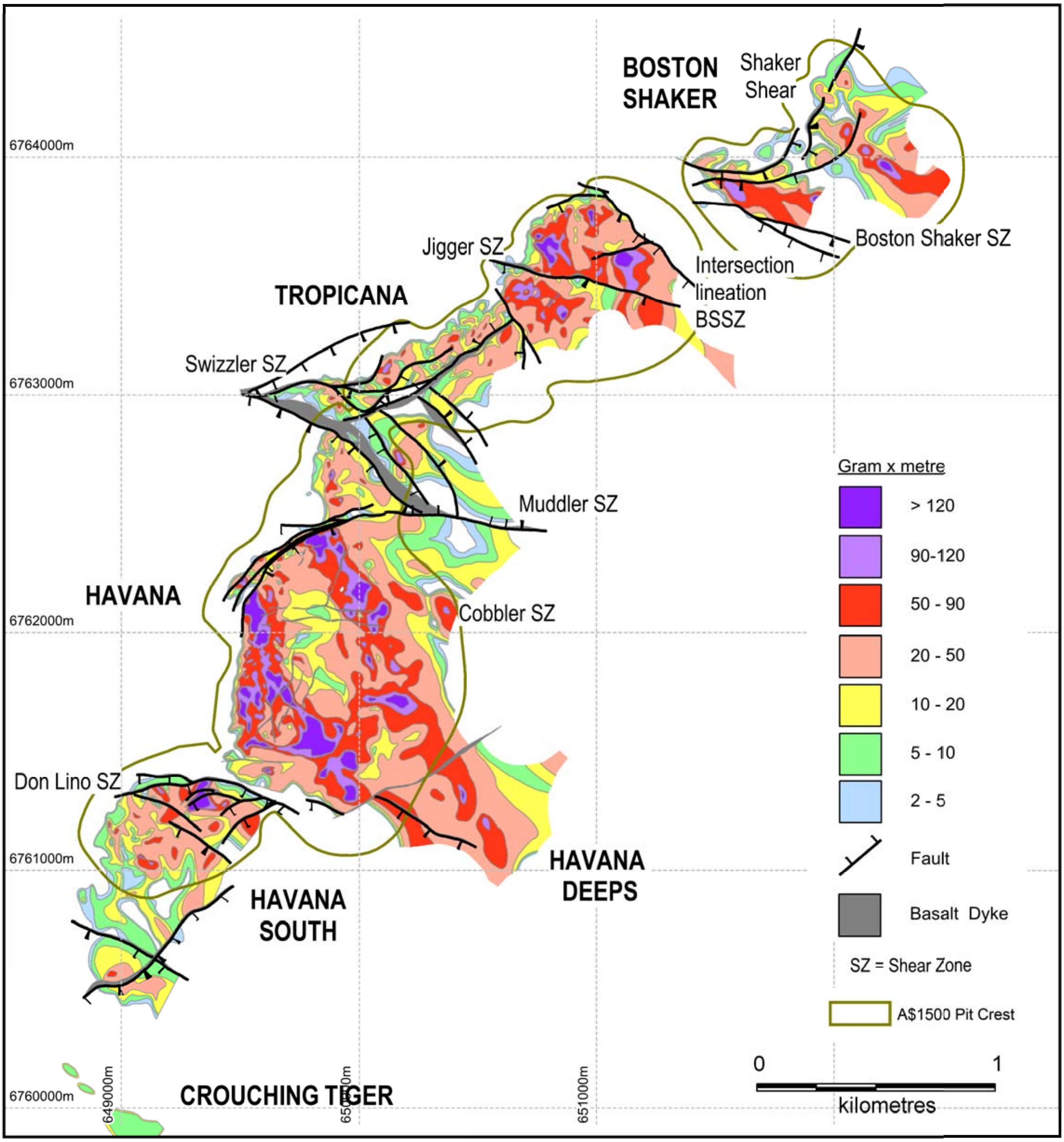

Fig. 3. Structural domains and mesoscopic shear zones of the Tropicana Deposit, superimposed on a grade (g/t) X thickness (m) plot. GDA/UTM grid

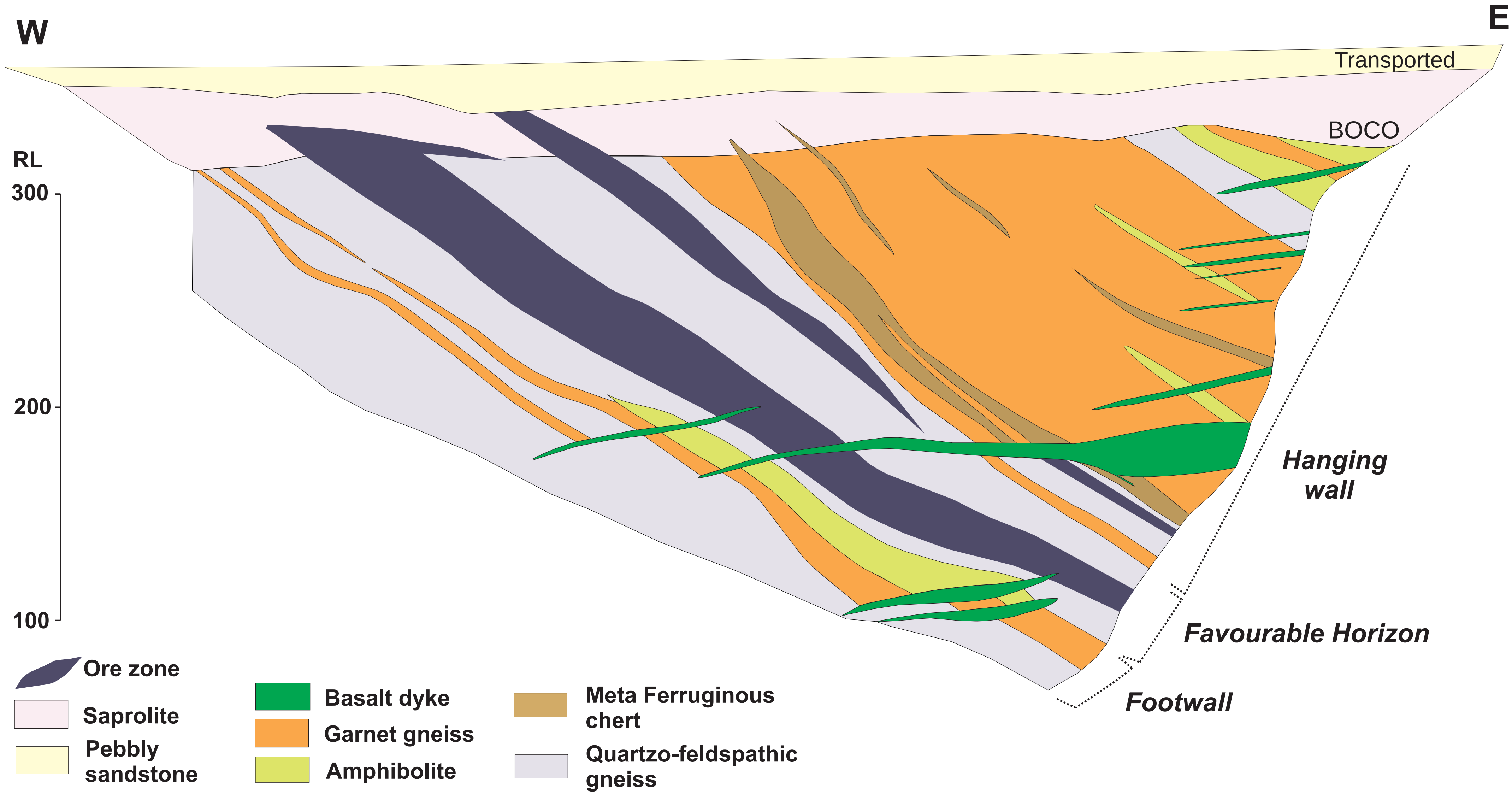

Fig. 4. Schematic EW cross section of the Tropicana Deposit (based on Spaggiari et al. 2011).

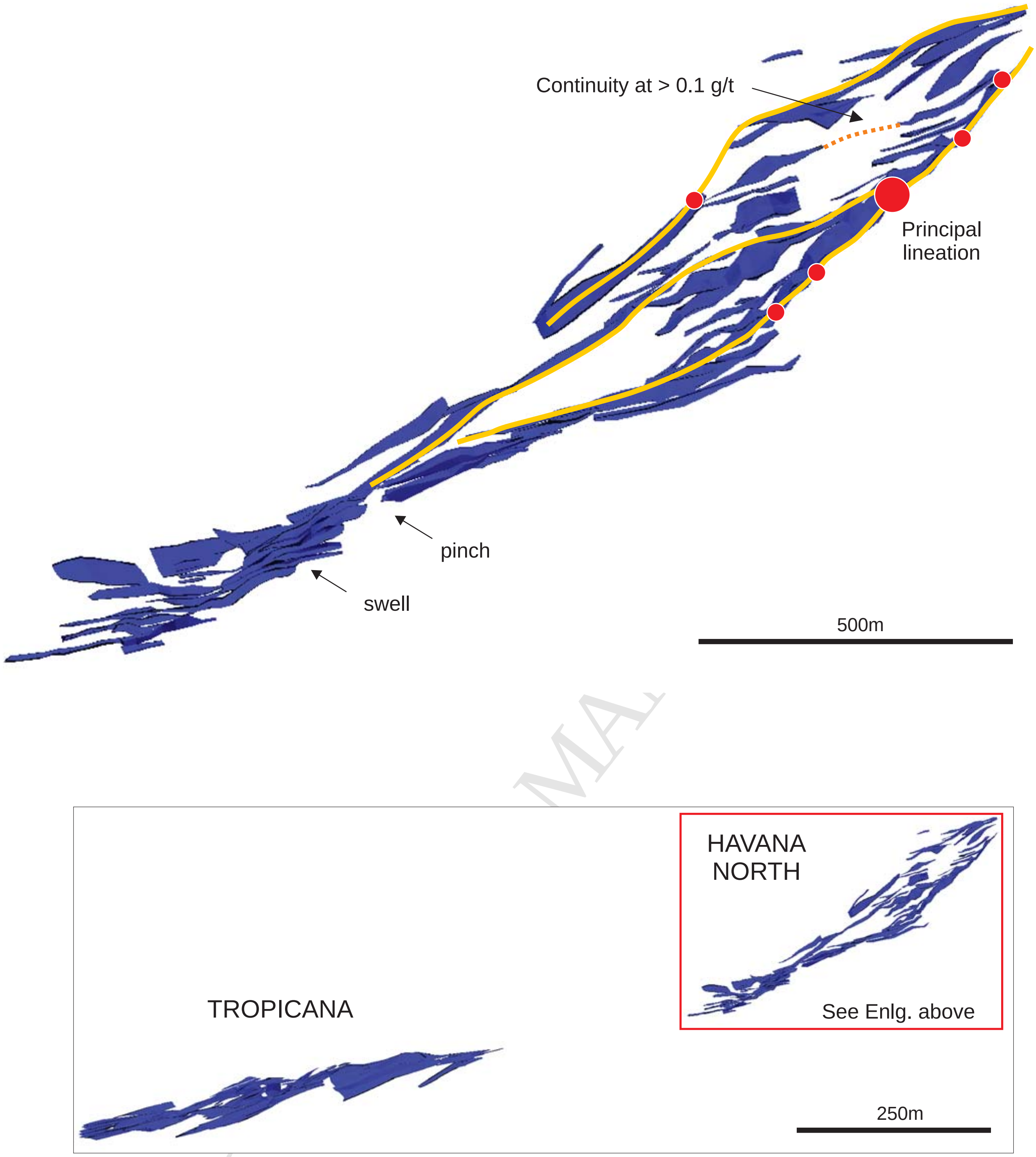

Fig. 5. NE-SW section (true scale). Blue shapes are delimited by > 3g/t. “Principal lineation” refers to the high grade ore shoots seen in the gram x metre plot of Fig. 3. High grade ore bodies pinch and swell.

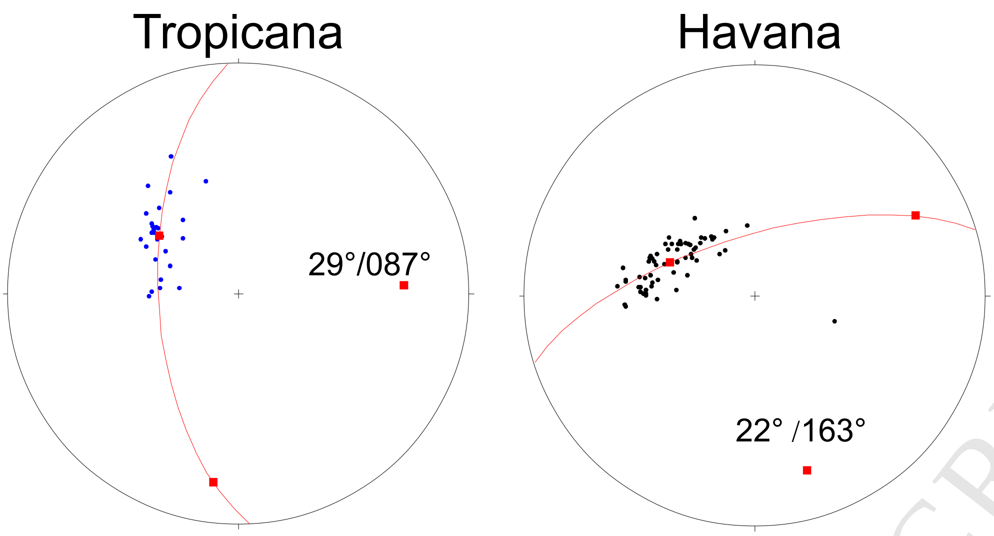

Fig. 6. Orientations of poles to high grade (>3 g/t) ore shells. A distinct difference is noted between the Tropicana and Havana domains.

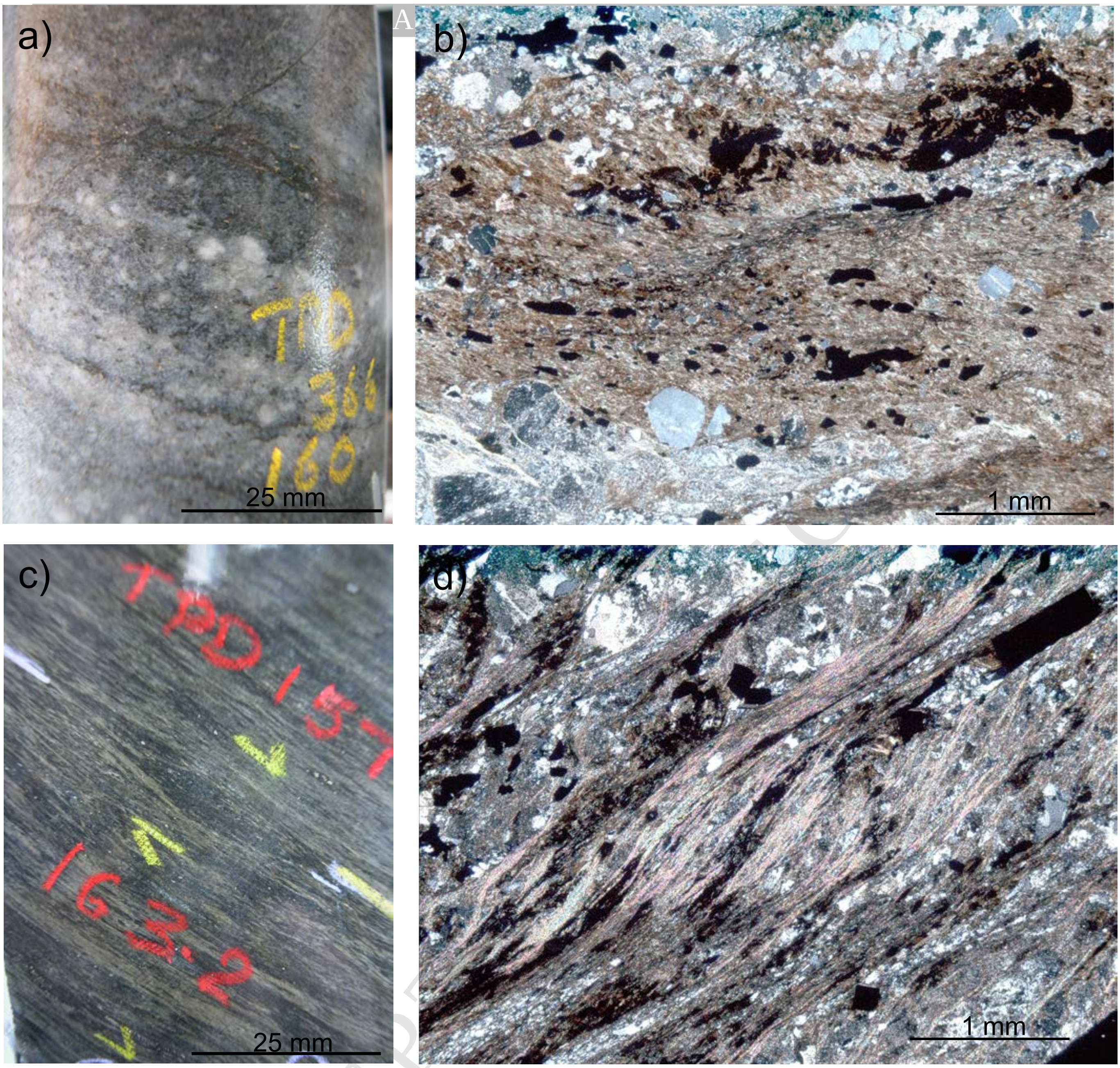

Fig. 7. Styles of Mineralization in the core.
a) Biotite-pyrite shear zone sub-parallel to gneissic banding, core TPD366, 160 m.
b) Biotite-pyrite shear zone (thin section). Foliation defined by biotite and pyrite gives clear top-to-the left sense of shear. Core TPD361A, 161 m, XPL (cross-polarised light).
c) Chlorite-sericite shear zone, core TPD167, 163.2 m. Asymmetric clast gives clear shear sense
d) Sericite shear zone (thin section). Spectacular SC fabrics defined by sericite and pyrite give clear top-to-the-right shear sense. TPD067, 143.3 m, XPL.

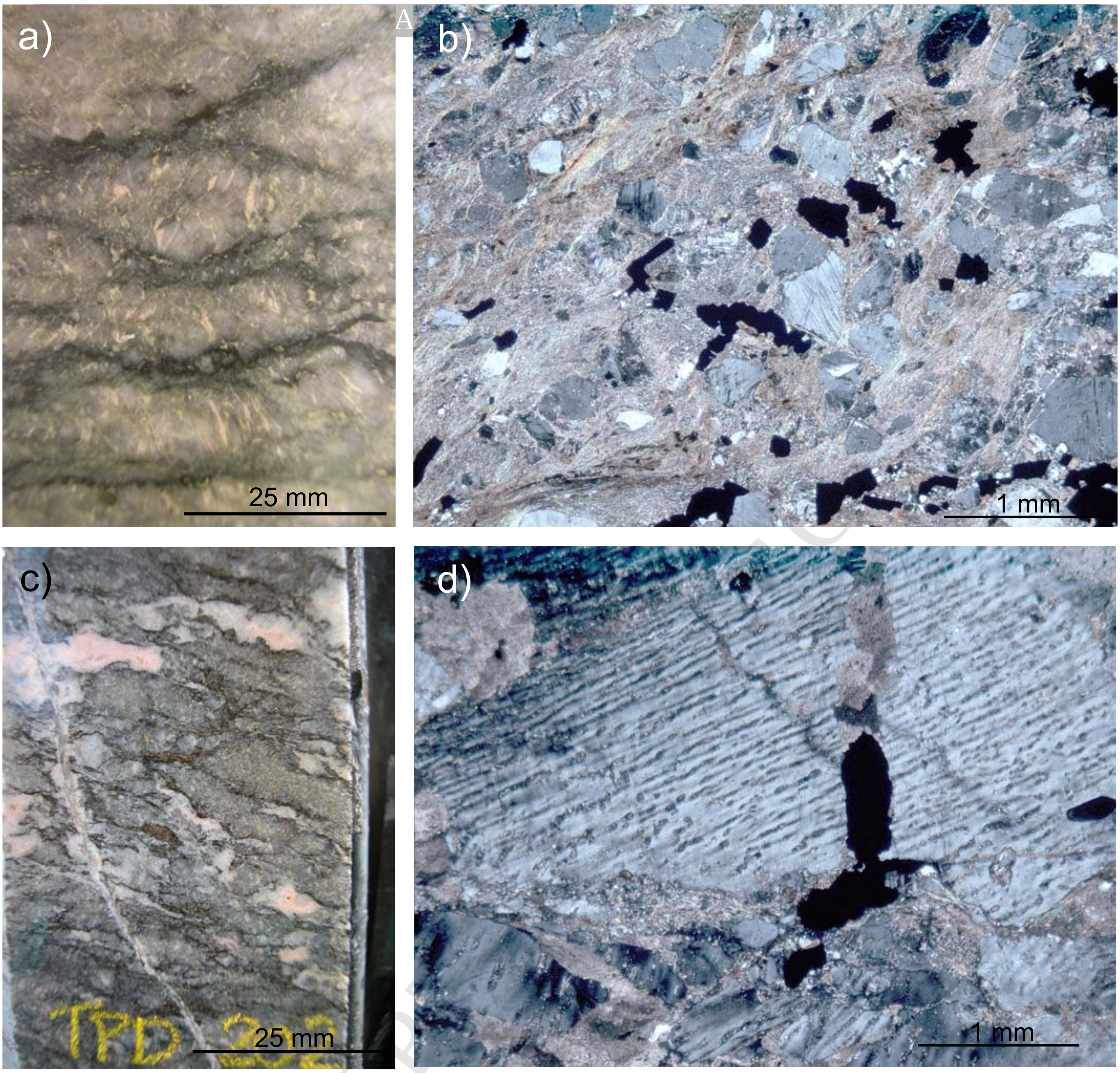

Fig. 8. Styles of mineralization in the core.
a) Solution seams with biotite anastomosing between lithons of feldspar with carbonate-filled extension fractures. TPD202, 281.9 m
b) Fragmentation and solution accompanying formation of carbonate-sericite-pyrite veins. TOD202B, 282.9 m, XPL.
c) More discrete formation of biotite lined solution seams and amorphous patches of carbonate. . TPD 202, 285.8 m
d) Extension microfracture in perthite grain, with filling of pyrite and carbonate. TPD202C, 283.9 m, XPL

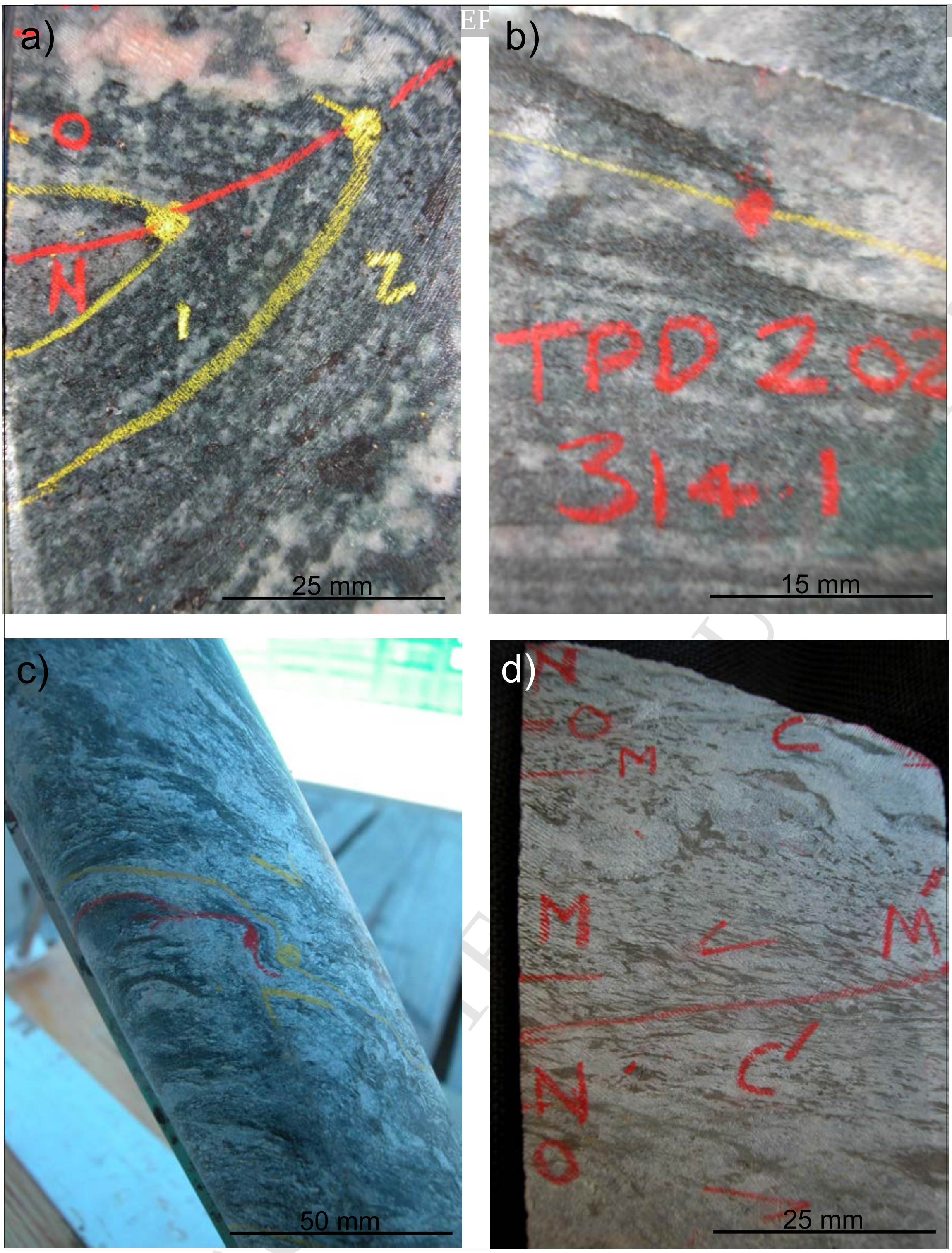

Fig. 9. Structural Features in core.
a) F1 Folds in gneissic banding. Yellow lines marks form surface, yellow spots are hinges and red line is hinge surface. TPD251, 222.7 m
b) Isoclinal F1 fold hinge of gneissic banding, TPD202, 314.1 m
c) Asymmetric F5 fold of gneissic banding and shear foliation. TPRC092D, 298.7 m
d) SC' defined by chlorite and sericite. Marking according to the scheme of Blenkinsop and Doyle (2010). TPD262, 162m

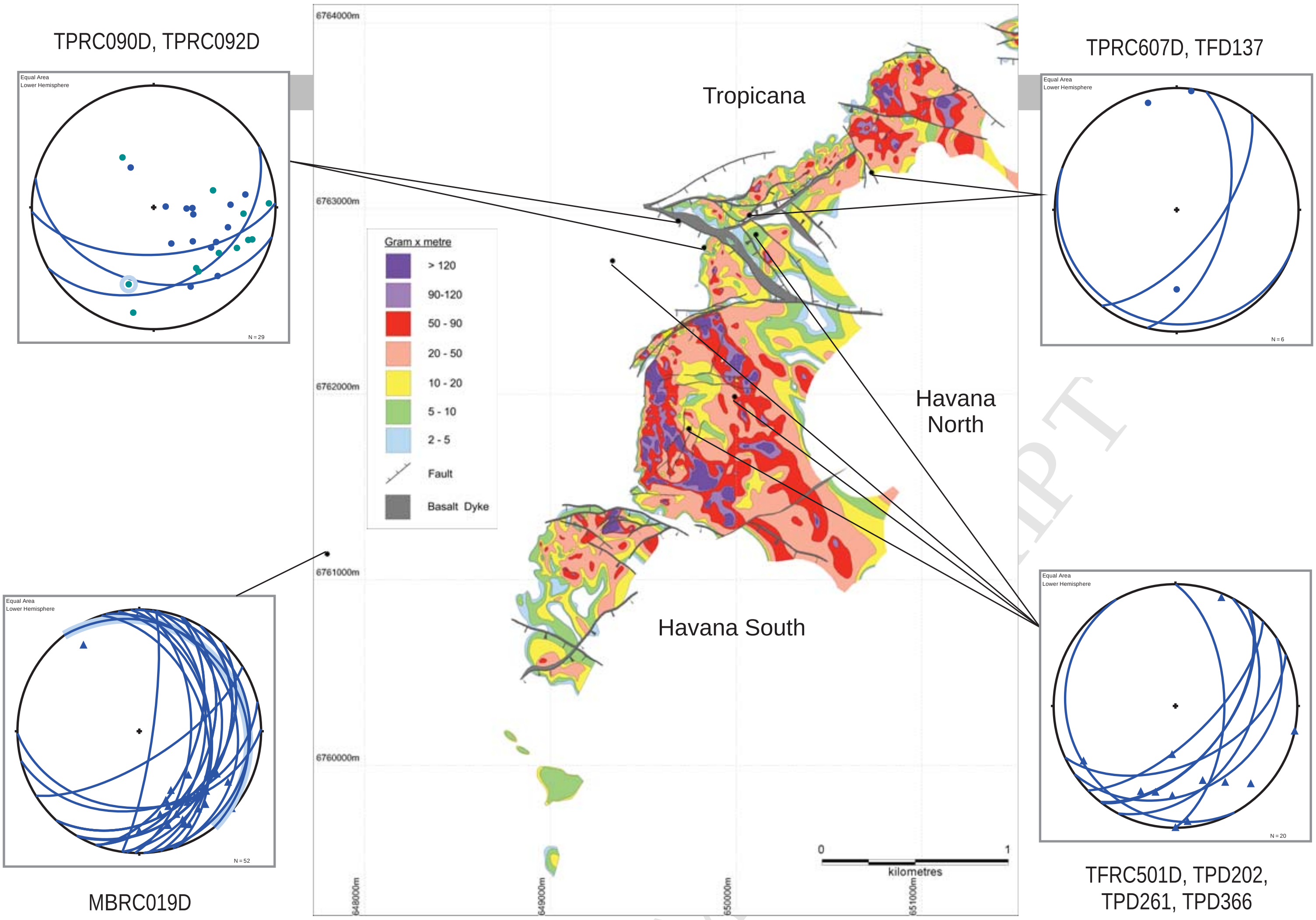

Fig. 10. Orientations of fold hinges and hinge surfaces, located relative to drillholes and structural domains. Folds in cores MBRC019D, TPRC607D, TFD137, TFRC501D, TPD202, TPD261 and TPD366 plunge moderately S to SE with E to SE dipping hinge surfaces. These are interpreted as F1 or F2 folds, because they are tight to isoclinal. Folds in cores TFRC090D and TFRC092D plunge moderately E to SE with S-dipping hinges surfaces. Many of these have dextral vergence (turquoise colour). These folds are located adjacent to the Boston Shaker shear zone and are F5 folds. Some of these folds which are not asymmetric could also be F3.

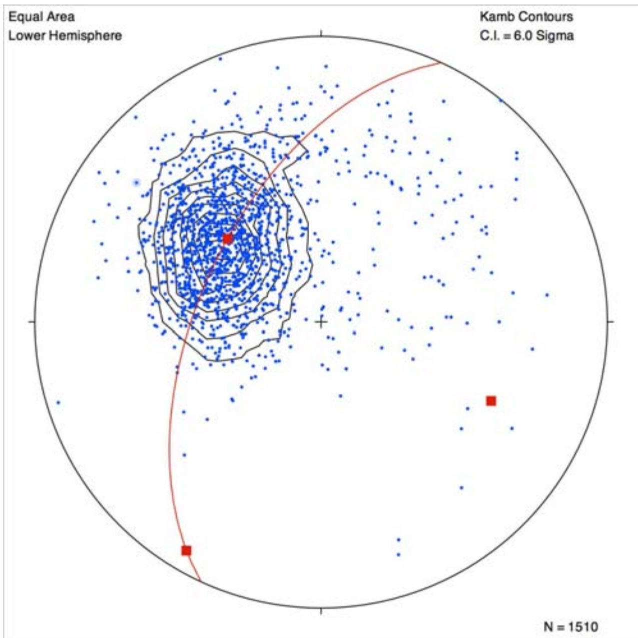

Fig. 11. Poles to gneissic banding (n = 1510) in the Havana domain. Cylindrical best fit gives a fold hinge plunging 35° to 115°. Kamb contours with a contour interval of 6σ , 3σ significance level.

Fig. 12. Geographic distribution of shear zones in ball-and-string plots. Great circles indicate shear planes: arrows indicate hangingwall movement. In most plots there are sub-parallel shears with different movement directions, testifying to reactivation.

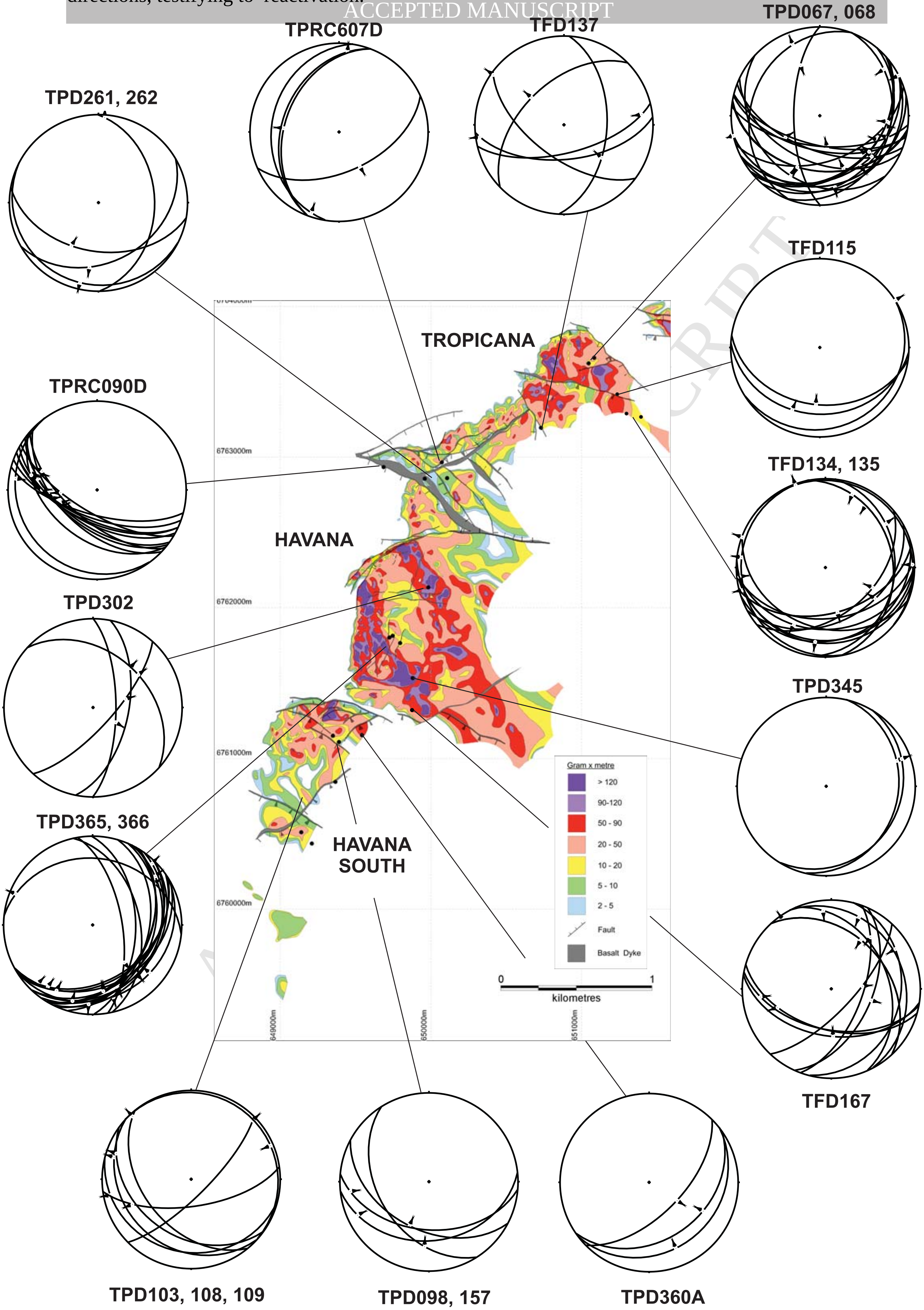

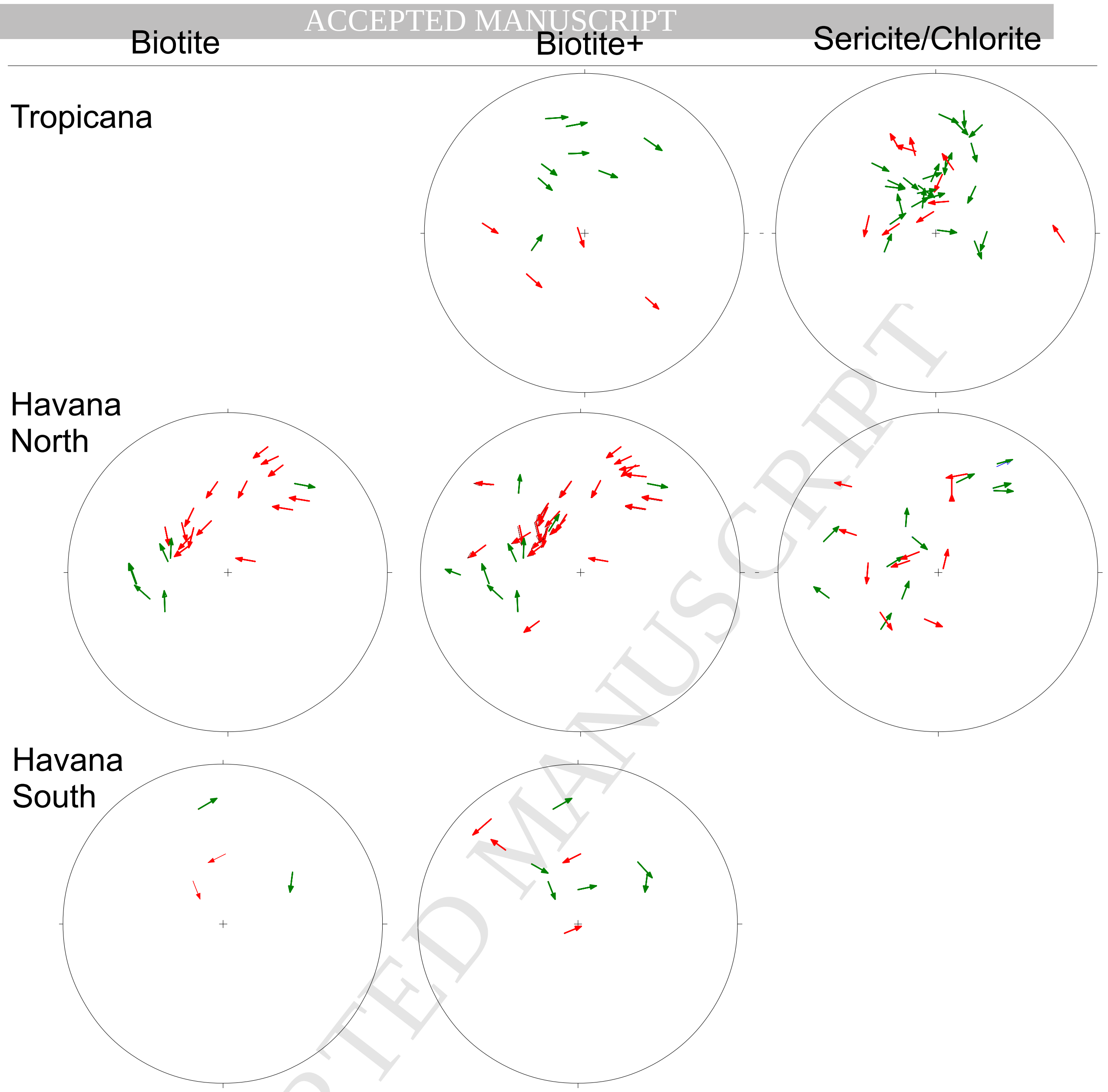

Fig. 13. Tangent lineation plots of shear zones separated by structural domain and by phyllosilicate mineralogy. Arrows indicate footwall movement. Dextral components in green and sinistral in red.

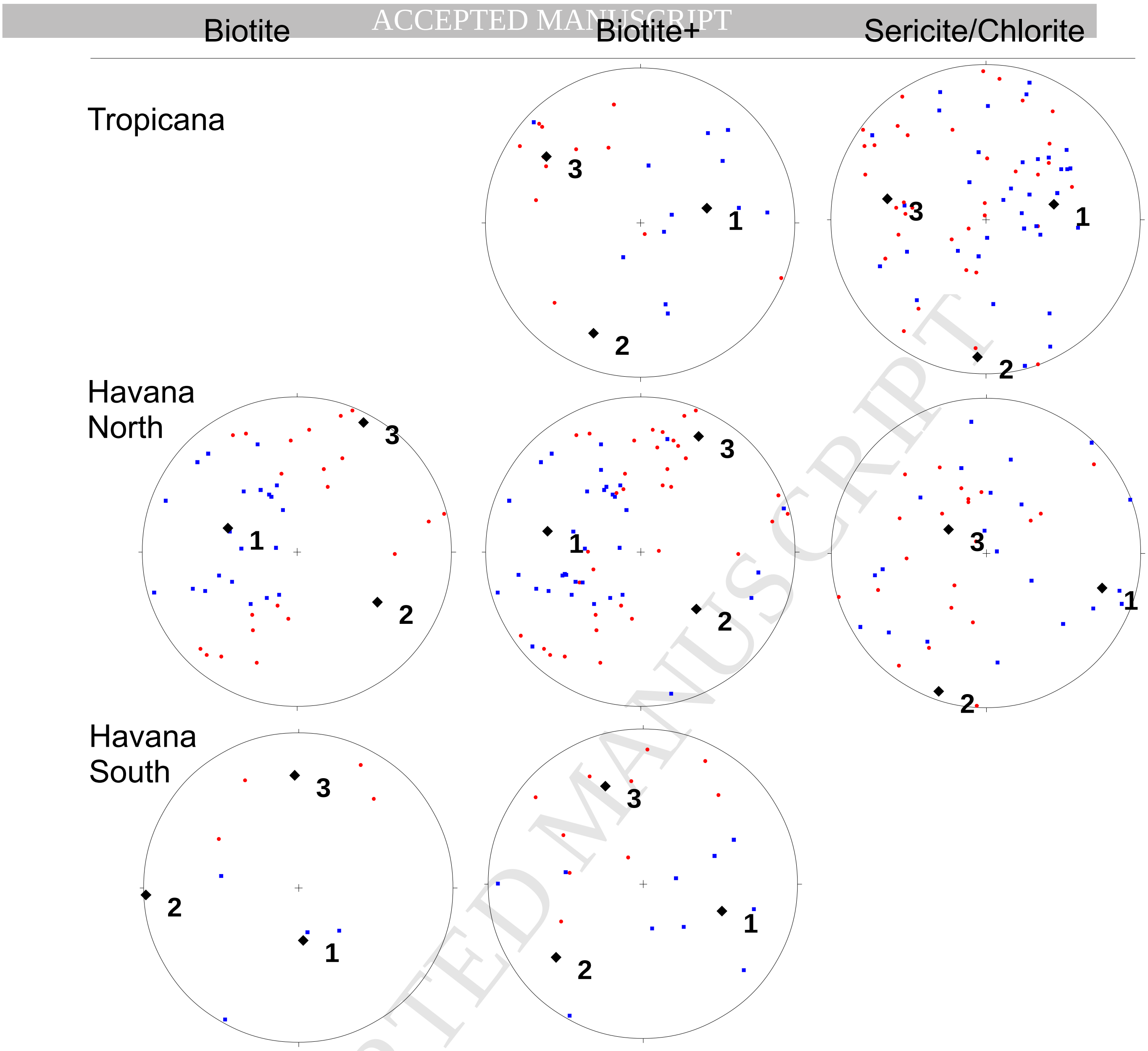

Fig. 14. Kinematic analysis of shear zones separated by structural domain and by phyllosilicate mineralogy. Red and blue dots are shortening and lengthening axes for individual shear zones respectively; 1, 2, and 3 are the linked Bingham axes for the distributions shown

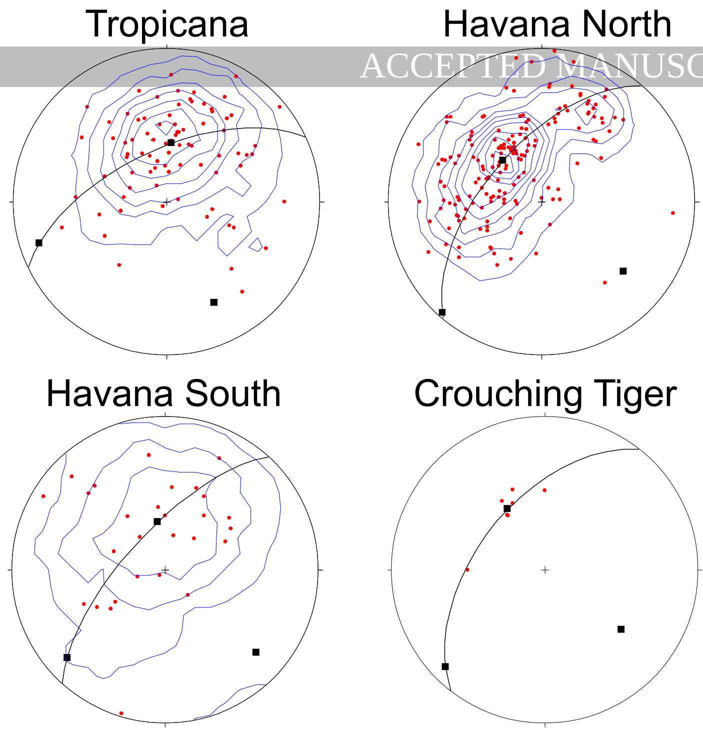
Tropicana
Havana North
Havana South
Crouching Tiger

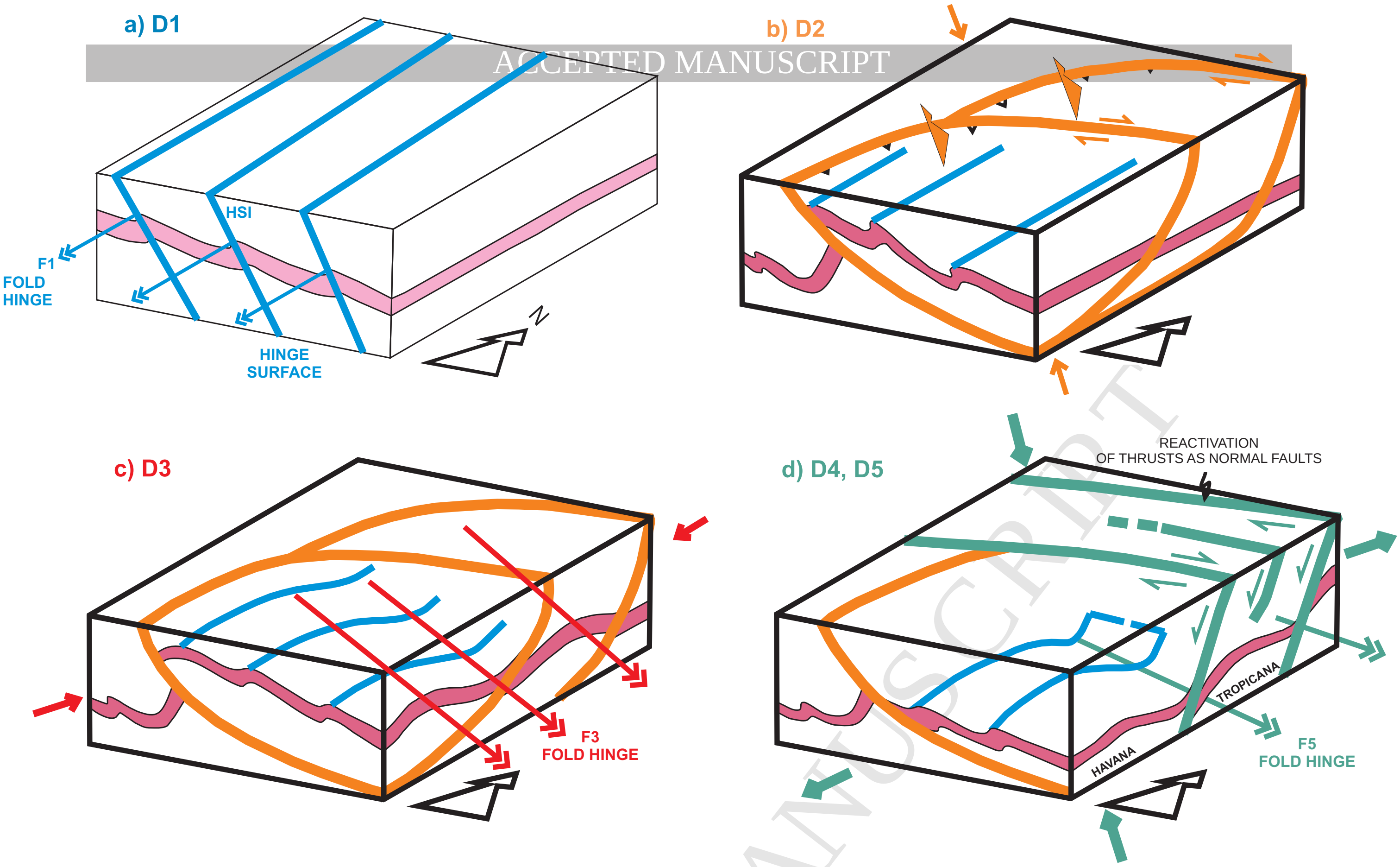

Fig. 16. Cartoon of the structural evolution of the Tropicana Gold Deposit

a) D1 is preserved as isoclinal folds and gneissic banding

b) D2: thrusting and folding is inferred from regional considerations

c) D3: the main mineralizing event, due to NE shortening

d) D5: The main reactivation

Supplementary Material for Blenkinsop and Doyle 2013.
Locations of Drillholes used in this study